Aalto-yliopisto
Aalto-universitetet
Aalto University

Master's Programme in ICT Innovation

Developing a portable, customizable, single-channel EEG device for homecare and validating it against a commercial EEG device

Máté Károly Tóth

Master's thesis
2023

Aalto-yliopisto
Aalto-universitetet
Aalto University

Author Máté Károly Tóth

Title of thesis Developing a portable, customizable, single-channel EEG device for homecare and validating it against a commercial EEG device

Programme ICT Innovation

Major Autonomous systems

Thesis supervisor Prof. Quan Zhou

Thesis supervisor Prof. Elena Troubitsyna

Thesis advisor(s) Prof. Pawel Herman

Thesis advisor(s) Tobias Wibble, PhD, MD

Collaborative partner Davide Frattini, MSc

Date 09.06.2023 **Number of pages** 49 + 11 **Language** English

Abstract

There are several commercial electroencephalography (EEG) devices on the market; however, affordable devices are not versatile for diverse research applications. The purpose of this project was to investigate how to develop a low-cost, portable, single-channel EEG system for a research institute that could be used for neurofeedback-related applications in homecare. A device comparison was intended to examine what system requirements such a system would need to achieve the secondary objective of developing a neurofeedback application that demonstrates the functionalities of the new device. A portable, single-channel EEG device prototype was realized that consisted of an amplifier module called EEG Click, a single-board microcontroller, an electrode cable, some disposable wet electrode pads, and a custom 3D-printed headband. Three pieces of software were developed: firmware for the prototype, two supporting computer applications for data recording, and visual neurofeedback. The neurofeedback application replayed a first-person view roller coaster video at a varying frame rate based on the theta band's mean power spectral density (PSD). The prototype was compared against a commercial device, InteraXon MUSE 2 (Muse). Technical measurements included determining the amplitude-frequency characteristics and signal quality, such as signal-to-noise ratio (SNR), spurious-free dynamic range (SFDR), and total harmonic distortion (THD). Furthermore, four physiological measurements were performed on six human test subjects, aged between 21-31 (mean: 26.0, std: 3.11), to compare the altered brain activity and induced artifacts between the two devices. The four tests were respiratory exercise, head movement exercise, eye movement exercise, and paced auditory serial addition test (PASAT), where each measurement included several epochs with various stimuli. After the recordings, PSD was calculated for each bandpass filtered epoch, then the spectra were split into theta (4-8 Hz), alpha (8-12 Hz), and beta bands (12-30 Hz).

The PSD values were averaged within each frequency band, and then these baseline-corrected mean values were the input for the repeated measures ANOVA statistical analysis. Results revealed that the amplitude-frequency characteristic of the prototype was low-pass filter-like and had a smaller slope than Muse's. The prototype's SNR, including and excluding the first five harmonics, was 6 dB higher, while SFDR and THD for the first five harmonics were roughly the same as Muse's. The two devices were comparable in detecting changes in most physiological measurements. Some differences between the two devices were that Muse was able to detect changes in respiratory activity in the beta band ($F_{(8,16)} = 2.510$, $p = .056$), while the prototype was more sensitive to eye movement, especially lateral and circular eye movement in theta ($F_{(2,8)} = 9.144$, $p = .009$) and alpha ($F_{(2,8)} = 6.095$, $p = .025$) bands. A low-cost, portable EEG prototype was successfully realized and validated. The prototype was capable of performing homecare neurofeedback in the theta band. The results indicated it is worth exploring further the capabilities of the prototype. Since the sample size was too small, more complex physiological measurements with more test subjects would be more conclusive. Nevertheless, the findings are promising; the prototype may become a product once.

Keywords Electroencephalography (EEG), Portable EEG, Single-channel EEG, Commercial EEG, Brain-machine interface, Prototype development

Acknowledgements

First, I would like to appreciate Marianne Bernadotte Centrum's support and the opportunity to work on this exciting project.

I want to express my deepest gratitude to Tobias Wibble for being the primary supervisor of the thesis and coordinating the project. This endeavor would not have been possible without his continuous support and general knowledge of academic writing and neurology.

I am incredibly grateful to Davide Frattini for similar reasons, guiding me through the project and helping me with psychology and statistical analysis-related topics.

I would like to thank Pawel Herman, my supervisor at KTH Royal Institute of Technology, for managing the project from an academic perspective, advising me on the thesis, and providing feedback.

I appreciate Ódinn Rúnarsson's help in introducing me to electroencephalography and neurofeedback.

I want to thank MentorSpace for supporting me with precious instruments for my measurements.

Finally, I would like to acknowledge all the others who contributed to this project or supported me during the most challenging times.

Thank you.

Stockholm, June 2023
Máté Károly Tóth

Table of Contents

List of Figures

List of Tables

List of acronyms and abbreviations

AC	Alternating current
ADC	Analog-to-digital converter
ANOVA	Analysis of variance
BCI	Brain-computer interface
CAD	Computer-aided design
CAGR	Compound annual growth rate
CT	Computer tomography
ECG	Electrocardiography
EEG	Electroencephalography / electroencephalogram
EMC	Electromagnetic compatibility
EMI	Electromagnetic interference
EP	Evoked potential
ERP	Event-related potential
FFT	Fast Fourier transform
fMRI	Functional magnetic resonance imaging
FPS	Frames per second
ICA	Independent component analysis
IIR	Infinite impulse response
IS 10-10	International 10-10 electrode system
MBC	Marianne Bernadotte Center
MEG	Magnetoencephalography
Mindwave	Mindwave Mobile 2
MRI	Magnetic resonance imaging
Muse	MUSE 2 Brain Sensing Headband
MVP	Minimum viable product
PASAT	Paced auditory serial addition test
PET	Positron emission tomography
PLA	Polylactic acid

POV	Point of view
PPG	Photoplethysmogram
PSP	Postsynaptic potential
RMS	Root-mean-square
RoHS	Restriction of Hazardous Substances
RSS	Root-sum-square
SFDR	Spurious-free dynamic range
SINAD	Signal-to-noise and distortion ratio
SNR	Signal-to-noise ratio
THD	Total harmonic distortion

Chapter 1

1 Introduction

The democratization of homecare is now more important than ever. Europe's population is constantly aging, and the demographic trend does not seem to change [1]. It has been proven that the demand for homecare highly correlates with age [2]. Changing lifestyles, shrinking families, and increasing female workforce participation has also reduced informal care rates and promoted formal homecare [3]. Accordingly, more and more people will depend on homecare in the near future [3]. However, homecare not only improves people's general health and well-being but addresses some sustainability issues. Homecare saves traveling costs, energy, and time for patients as well as healthcare professionals, whose time is invaluable due to their limited number. One of the positive impacts of the Covid-19 pandemic was that it accelerated Europe's digital transformation. A recent survey shows that clients and patients prefer homecare over visiting doctors [3]. To fulfill these needs, there is a high demand for new medical devices that can be used at home; however, their availability is sparse compared to clinical systems. Fortunately, technology constantly lowers the barriers to entry and promotes product alternatives; consequently, new homecare devices appear on the market every day. In mental homecare, electroencephalography (EEG) is gaining more relevance as it enables to manufacture of low-cost portable devices that can record the brain in real-time [4]. In fact, EEG is the most widely used mobile method for monitoring the brain [5].

Electroencephalography is the potential difference between various parts of the cerebral cortex area and is a non-invasive method used to examine and record brain activity [6]. The first EEG measurement was done in 1924 by German engineer Hans Berger [7]. Berger's electroencephalogram (EEG) was quite simple compared to the modern EEG systems, which are digital nowadays as these systems consist of a computer and specific software which can perform standard EEG, video EEG, ambulatory EEG, or long-term monitoring [6]. Although electroencephalography is not considered a state-of-the-art method anymore, clinical EEG is still widely utilized to study the brain of ill patients, which can reveal diseases, such as epilepsy, Alzheimer's, or brain tumors, or it also can give insight into head injuries, strokes, or sleeping disorders [8]. Besides clinical usage, EEG is an appealing method for both laboratory and research applications due to its non-invasive and reproducible nature and because the tests are easy yet relatively cheap [6]. Moreover, EEG devices are gaining more popularity in homecare and meditation. Over the decades, the EEG market has constantly been changing, and currently, it drifts towards consumer-grade EEG systems [7].

The global EEG equipment market was worth over 1.4 billion USD in 2018 [9], and it is expected to reach 1.8 billion USD by 2028 [10]. According to a more optimistic estimation, the market would grow to 2 billion USD in 2026 with an expected Compound Annual Growth Rate (CAGR) of 4.5% (calculated from 2019 to 2026) [9]. By product type, the market can be segmented into integrated EEG, portable EEG, and EEG accessories categories. Integrated EEG apparatuses are extremely complex systems, quite expensive, and typically meant to be used in a clinical environment. It usually takes much time to set up the equipment, which is done by trained medical technicians [6]. On the other hand, portable devices are primarily used at homecare and ambulatory centers [10]. Portable devices have the advantage of reduced costs (both manufacturing and operating), higher mobility, smaller size and weight, shorter installation time, and reduced traveling time for patients. One of their most significant advantages is that they can perform data recording at home, where people may be expected

to respond in a more natural fashion, mitigating the effects brought on by the clinical intervention. Standalone devices had the highest share of the EEG market in 2020; however, the demand for portable devices is expected to increase in the upcoming years [10].

1.1 Problem

There is a high demand for portable, easy-to-use EEG devices that patients can use at home [11]. There are several commercial devices on the market that meet the criteria to some extent; however, they are too generic for versatile medical applications because they are not customizable - for example, they have fixed electrode placement, their bandwidth is too narrow for a specific application or their sample rate is not adjustable [7]. Moreover, these devices are often "black boxes"; their inner functions cannot be reached or even known publicly, and they offer few interfaces to interact with. An issue that typically exists for low-end devices is that their outputs are already filtered, and raw data cannot be acquired directly. There are higher quality instruments on the market that overcome most of these problems, but they are rather expensive, and yet they still do not have medical certifications. Therefore, there is a need for low-cost, customizable, versatile, portable EEG systems designed for diverse research and treatment applications.

1.2 Purpose

The purpose of this project was to investigate how to develop a low-cost, portable, single-channel EEG system for a research institute that could be used for neurofeedback-related applications in homecare. The prototype was supposed to be customizable, easy to use, relatively cheap, yet reasonably robust to noise and artifacts. The societal value of the project was that it supports the democratization of homecare, enables home treatment of several brain illnesses, and might bring more insight into the healthy human brain over long-term data recording. The engineering interest of the project was to realize such a device, while the scientific interest of this project was investigating the design process, measuring the prototype's capabilities, and exploring its viability as an open-access research tool. In more detail, the research aimed to validate the proposed prototype by comparing it against a commercial-grade EEG system, evaluate the prototype’s suitability for neurofeedback, and explore design considerations for an affordable homecare brain-computer interface (BCI) system. The assumption was that the prototype could accomplish the same functional tasks, such as neurofeedback or long-term data acquisition, as a low-cost, regular commercial-grade EEG device. Provided that the prototype had similar characteristics and technical properties as a previously scientifically validated commercial device, the custom in-lab device would also be suitable for future research and treatment applications. The comparison focused on assessing signal quality and investigating fundamental brain signals under different stimuli and artifacts. Additionally, the research aimed to explore the usability requirements and technological solutions involved in designing an affordable at-home BCI system that can support neurofeedback applications.

Specifically, widely available consumer-grade EEG systems refer to general-purpose commercial devices as opposed to EEG systems designed for clinical and research purposes. Low cost was defined as the devices' consumer price was under €500 (the typical price range is €200-300). Signal quality meant examining the frequency response of the system, and assessing the quality of the time domain signals by the most typical metrics, such as signal-to-noise ratio.

1.3 Objectives

Two primary objectives and a secondary objective were defined for this project.

1.3.1 Primary objective I.

The first primary goal was developing the prototype of a cheap, easy-to-use, portable, versatile, and customizable single-channel EEG device that patients can use at home. The primary application would be homecare rehabilitation for motion sickness, visual vertigo, and other motion-related disorders by forming a neurofeedback system with the patient and a computer. Alternatively, it could be used to gather long-term data from healthy participants.

The prototype could eventually become a commercial product, so the proposed device developed as part of this thesis could be considered the minimum viable product (MVP) of the final product, thus performing fewer functions than its commercially available counterparts. Later, however, the system can be extended to have more features and solve multiple problems. While such inclusions are not within the scope of the present thesis, they may prove valuable for planning the future development of the device.

1.3.2 Primary objective II.

The second primary objective was to address the research aim of the study. The first part was to validate the prototype and compare it against a commercial EEG system. The comparison aimed to assess the qualities of the two devices by various technical and physiological measurements (experiments), where the latter was supposed to be performed on human subjects. Besides, the scientific purpose of the thesis was to determine whether it is worth or not to explore the capabilities of the in-lab device further. Finally, concluding the findings, evaluating the prototype suitability for neurofeedback, and exploring design considerations.

1.3.3 Secondary objective

A secondary objective was to develop a simple neurofeedback (NFB) application for the validated device to demonstrate its capabilities. The demo application had no new form of validation processes as that would have involved weeks of training regimen, which was out of the project's scope.

1.4 Delimitations

The validation output was an explorative study; it was not intended to provide detailed quantitative results but to determine the feasibility of developing an in-lab EEG device and to allow pilot trials that may guide future developments. Therefore, statistical procedures may only be viewed as indicative of specific trends, as insufficient statistical power had been achieved to form concrete conclusions.

The neurofeedback application was intended to demonstrate the possible use of the in-lab EEG device and was not validated as a rehabilitation tool at this stage. Instead, it aimed to lay out the foundation of a possible homecare application. Therefore, testing and validation of the neurofeedback application were out of this project's scope as they would be too complex and time-consuming.

1.5 Outline of the thesis

The upcoming chapters of the thesis are structured as follows:

Chapter 2 presents the background of the project.

Chapter 3 explains the prototype development and components of the system.

Chapter 4 introduces the materials and methods of the thesis.

Chapter 5 presents the results.

Chapter 6 discusses the findings.

Chapter 7 concludes the thesis.

Chapter 2

2 Background

2.1 Studying the brain

The brain has been studied for quite some time, as the history of neuroscience can be traced back to antiquity. According to Herodotus, the ancient Egyptian civilization had medical experts specializing in head injuries [12]. The Egyptians described the cerebral cortex first, and they were aware of illnesses and medical conditions such as migraine, epilepsy, stroke, tetanus, and Bell's palsy more than 3500 years ago [12] [13]. Neuroscience has evolved stupendously since. Several milestones in its history are noteworthy, such as the black reaction coloring technique of the neural cells, Cajal's neuron doctrine, and the adaptation of medical imaging [13].

Cajal's principles of neuronal theory explain that the nervous system is built up of neural tissues composed of individual cells, neurons, and neuroglia [14]. Nervous tissues can be found in the human brain, the spinal cord (central nervous system), and the peripherical nerves (peripherical nervous system). Neurons are electrically excitable cells; therefore, they communicate with electrical signals. Their function is to generate and propagate nerve impulses. These individual cells can be decomposed into the soma (cell body), dendrites, and axon. The soma is the cell's center, containing the nucleus and other major organelles [15]. The dendrites are the extensions that gather the impulses and transmit them to the soma, while the axon carries away the impulses from the soma and regenerates them [15]. Neuroglia, also known as glial cells, are not directly involved in signal propagation, but they support the functioning of the neurons. Inside the neurons, the signal transmission is performed by voltage-gate ion channels that create action potentials by reversing the resting membrane potential [15]. This traveling action potential changes the polarity of the membrane along its way until it reaches the end, where it stimulates other neurons via neurotransmitters. Neurotransmitters are specific molecules that transmit signals between the nerve cells. When a strong enough chemical input reaches the synapses, the related neuron's membrane potential will reach the threshold; hence the neuron will fire an action potential [16]. Because of the threshold, action potentials function basically as binary signals: either there is a signal with a certain amplitude, or there is no signal at all; the amplitude of the action potential is not proportional to the magnitude of the stimulus. This phenomenon is often referred to "all or none" principle in the field of physiology. The lifetime of the action potentials is relatively short; typically, action potentials last for 1 ms [6]. Neural oscillations are the summarized activity of millions of nerve cells. Action potentials contribute little to neural oscillations; the main sources of brainwaves are the postsynaptic potentials (PSP) [6]. PSPs are temporary changes in the membrane potential of the neurons, and they can be excitatory or inhibitory. Postsynaptic potentials do not have a threshold, they can aggregate limitlessly, and their amplitude gradually increases as the magnitude of the stimulus increases. Moreover, postsynaptic potentials last longer than action potentials, roughly 10 – 40 ms; therefore, they have more time to accumulate, synchronize and generate large enough electric fields that can be recorded by electrophysiological systems [6].

2.2 Neuroimaging and electrophysiological methods

Engineering sciences have been developing in parallel with neuroscience. As a result of this, new technologies and methods have emerged to assist in the work of clinicians and researchers in the medical field. Besides electrophysiological methods, neuroimaging techniques are exceptional tools for studying the brain. Neuroimaging technologies are widely used to gain insight into brain anatomy, physiology, chemistry, and electrical activity levels [17]. They offer invaluable tools to diagnose diseases or detect head injuries. Neuroimaging refers to technologies when the output is either a structural image such as the computerized tomographic scanner (CT scan) or magnetic resonance imaging (MRI); or a functional image such as positron emission tomography (PET) or functional magnetic resonance imaging (fMRI) [18]. Electroencephalography and magnetoencephalography (MEG) are typically considered to be electrophysiological techniques because they measure the electromagnetic activity of the brain directly; however, sometimes they are also referred to as neuroimaging because their output data can also be visualized, especially when used in high-density montages. Electrophysiology examines the electrical activity of neurons and the related cellular processes which generate these signals [19]. Electroencephalography has the best temporal resolution among the previously mentioned techniques, and its typical temporal resolution is around 1 ms [20]; however, it has the worst spatial resolution. The spatial resolution can be improved by increasing the number of electrodes in the montage. Scalp electroencephalogram systems with 19 electrodes have a spatial resolution between 22-37 cm3, while EEG systems with 129 electrodes have 6-8 cm^3 [21]. In contrast, fMRI excels at spatial resolution (3-4 mm) but performs poorly in temporal resolution (1 sec) [20] [22]. While functional magnetic resonance imaging registers the local cerebral blood flow, electroencephalography directly records the neurons' electrical activity [20] [22]. In simple medical systems, high spatial resolution is often not required, but high temporal resolution is essential to study the dynamics of neural signals. The advantage of EEG resides in its simple system structure, low cost, and high temporal resolution. Electroencephalography offers a unique opportunity to gain insight into the brain's ongoing processes and directly measure something simple yet useful. Accordingly, EEG is still relevant today; furthermore, it has the potential to outshine state-of-the-art methods in some special use cases.

As was stated earlier, EEG surveys the summarized activity of millions of nerve cells as neural oscillations. Neural oscillations of different frequency ranges, also known as brainwaves or rhythms, can be associated with different behavioral and functional mental states [20]. Four classical frequency bands of EEG can be distinguished: the delta, the theta, the alpha, and the beta waves [6]. Beyond the traditional EEG frequency bands is the fifth type of brainwave, the gamma wave. They became relevant for research recently with the appearance of modern, high-quality digital EEG systems [6]. Delta band covers the slowest brainwaves (0.3 - 4 Hz), typically associated with deep sleep and dreaming [23]. Theta waves (4 - 8 Hz) are associated with drowsiness, a deeply relaxed state, and inward focus. Alpha waves (8 - 13 Hz) are responsible for the alpha rhythm that causes an especially relaxed mental state with passive (internal) attention. Beta waves (13 - 30 Hz) are responsible for cognitive processes, external attention, and anxiety. Finally, gamma waves (30 - 80 Hz) are the most rapid brainwaves associated with a highly concentrated mental state. Recent studies showed that every human has a unique brain wave pattern [23]. A summary of the five brainwave types can be seen in Table 1.

Table 1 - Summary of the brainwaves [6] [23]

Neural oscillation	Frequency range	Associated mental state and behavior
Delta wave	0.5-4 Hz	Sleeping, dreaming
Theta wave	4-8 Hz	Drowsiness, relaxed state, inward focus
Alpha wave	8-12 Hz	Relaxed state, passive attention
Beta wave	12-30 Hz	Cognitive processes, external attention, anxiety
Gamma wave	30+ Hz	Concentration

Since electroencephalography has a relatively high temporal resolution, it is a extraordinary tool for studying the brain's neural oscillations and examining evoked potentials (EP) and event-related potentials. Evoked potentials are electrical signal responses of the nervous system to external stimuli [24]. Event-related potentials are also direct responses generated by the nervous system. The difference between ERP and EP is that event-related potentials tend to have higher latency and correlate with higher cognitive processing [25]. It is worth mentioning that some scientific publications do not distinguish between the ERP and the EP; therefore, both of them will be referred to as evoked potentials henceforth.

In contrast to evoked potentials, amplitude spectrum, power spectrum, and power spectral density (PSD) examine the signal in the frequency domain instead of the time domain. Consequently, local temporal information is lost, and only global temporal information is preserved. Frequency domain examination is fundamentally a statistical analysis that helps to understand the behavior of the signal and system. Fast Fourier Transform (FFT) is a computationally efficient algorithm to calculate different spectra. Power spectral density is essentially the power spectrum of the signal normalized by frequency (whitened); therefore, its unit of measurement is V^2/Hz. In some cases, both local time and frequency domain information should be acquired and extracted from a raw signal simultaneously. Subdividing the signal into shorter durations, using various windowing techniques, and utilizing a short-time Fourier transform could be a possible solution. Alternatively, a wavelet transform can be used for the analysis that essentially convolves the original signal with a wavelet function, such as the Morlet wavelet. The output of the transformation is often a graphical 2D or 3D spectrogram. It is noteworthy to mention, however, there is always a trade-off between time and frequency resolution, which is due to the time-frequency uncertainty principle.

2.3 Commercial-grade EEG systems

Changing trends could be observed in the examination of the human brain in the past decades, as engineering studies increased compared to psychological and physiological investigations [7]. Traditional EEG systems, typically used in clinical environments, are complex, high maintenance, difficult, and time-consuming to set up. They are not ideal for general purpose, or ordinary uses, therefore, demand started to increase for commercial EEG systems. Technology broke down the barriers, and the market could supply the demand with novel, wireless, portable, higher-quality, multi-channel consumer-grade EEG systems [7]. Their major selling points are affordability, portability, and ease of use, and these new devices are expected to have similar efficiency, accuracy, and signal quality as their clinical and research tool counterparts [7]. Hundreds of validation studies focused on comparing the performance of commercial-grade devices with medical and research-grade EEG systems [7].

A particular study for commercial-grade EEG systems used as research tools reviewed 91 academic papers which covered 18 different devices [7]. The study focused on four major different application areas of the devices, which were BCI, cognition, education, and gaming. The conclusion was that signal quality is still a serious concern particularly due to the lower number of electrodes, and artifacts induction of the portability nature of devices [7]. Regardless, countless research studies used commercial-grade EEG to overcome the disadvantages of traditional EEG systems, such as high cost, long setup-up time, and discomfort [7]. The commercial-grade EEG devices are targeted at home and school general use cases, besides low-budget research applications. The study also revealed that researchers were able to simultaneously hand out more devices to patients, and the brain signal can be recorded for a longer period, which proved to be invaluable features of the commercial devices [7].

Commerical-grade EEG devices may emphasize one of EEG's hidden advantages, the potential simplicity and low cost when used in a small number of electrode montages. While high-density electrode montages are required for increased spatial resolution in research and clinical applications, neurofeedback and BCI applications try to optimize the number and the location of the electrodes to reduce manufacturing costs and decrease setup time [5]. Reducing the electrode number and quality opens opportunities for the more simple, portable, single-channel EEG devices, which have one active electrode channel. One may suggest that the highest trade-off cost is less accurate data acquisition. For multi-electrode EEG systems, independent component analysis (ICA) and post-recording (offline) re-referencing are standard practices to help extract the valid signal and significantly increase the signal-to-noise ratio (SNR) [26]. Unfortunately, single-channel devices do not have this option. Despite the lower quality data, single-channel portable EEG devices are gaining more and more popularity among researchers. In the age of big data, the contribution of these devices for data collection could be invaluable for the health of society. Machine learning algorithms can be fed with this vast amount of data to find patterns and predict possible illnesses or improve people's general well-being. Portable EEG systems with few electrodes will likely play a vital role in democratizing homecare treatment. Neurofeedback (NFB), brain-computer interfaces (BCI), homecare diagnostics, and therapies are gaining more relevance in non-clinical and mobile environments [5]. EEG is the most widely used technology for the monitoring and alteration of brain activity in these environments because of the lightweight and compact state-of-the-art electronics.

A brain-computer interface is a digital system that can acquire, examine and interpret human brain waves [27]. BCI offers a new communication method without using the conventional output pathways of peripheral nerves and muscles. Instead, BCI strictly utilizes the signals of the central nervous system. The brainwaves can be directly translated into computer commands, therefore, BCI can help disabled people typically affected by neuromuscular disorders communicate [27]. Besides, there are various applications for BCI, such as neurorehabilitation, controlling objects (e.g. robots or wheelchairs), or interacting with the environment in other ways. Typically, a BCI system has signal acquisition, feature extraction and translation, and signal output functionalities [27]. Most BCI is based on EEG, which record brain signal originating from PSP. However, an EEG machine is not a BCI on its own, because EEG does not generate an output that interacts with the environment [27]. EEG but realizes the signal acquisition functionality of the BCI system. Nevertheless, when the functionalities of the EEG system are extended by a computer, it can be considered a BCI. A relevant application of BCI from the perspective of this study is neurofeedback.

Neurofeedback is a biofeedback technique to recondition the brain and retrain brainwave patterns [28]. Biofeedback is a method of providing physiological information to the subject in real-time [29]. Two types of biofeedback can be distinguished: direct feedback, which displays the numeric value of the chosen biomedical variable, and transformed feedback, which outputs an auditory or visual signal based on the measured biological variable [29]. NFB is often called EEG biofeedback when brain waves are examined and the signals are acquired by EEG systems. Neurofeedback may prove a valuable treatment alternative to medicine as research shows that it can effectively treat uncontrolled epilepsy, anxiety, post-traumatic stress disorder, learning disabilities, stroke, depression, motion sickness, and problems with physical balance [28]. Besides clinical and research uses cases, NFB is becoming more popular for meditation, pain management, and the enhancement of athletic and musical performance applications [30]. The democratization of homecare also involves the spread of simple neurofeedback-capable EEG devices.

Chapter 3

3 Prototype development

3.1 Overview of the neurofeedback system

As stated earlier, the primary purpose of the prototype was to perform homecare neurofeedback training. The neurofeedback application was designed to treat motion sickness and visual vertigo by replaying a video at varying speeds. The physiological input of the transformed feedback was the mean PSD of the theta band. The proposed visual neurofeedback system would consist of the EEG prototype with electrodes, a PC with a monitor, and a human subject. Figure 1 shows the diagram of such a neurofeedback system. Since the prototype was part of the neurofeedback system, which processed and interpreted information, the system can be considered a real brain-computer interface.

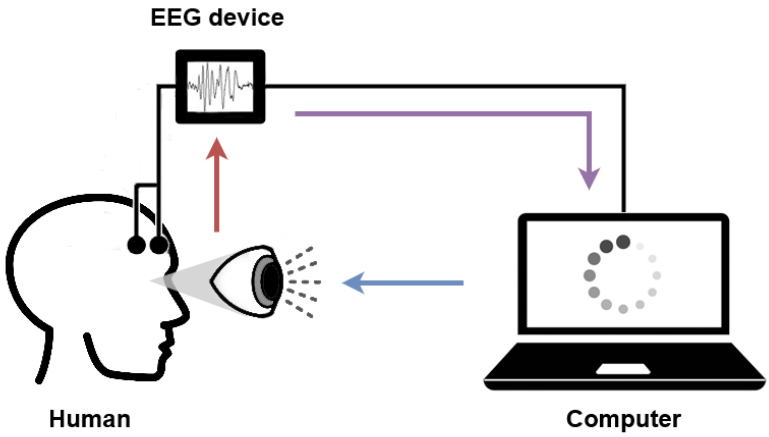

Figure 1 – A simple visual neurofeedback system. In the figure, the red arrow indicates that the EEG device records the voltage levels of the brain oscillations. The purple arrow indicates that the device transmits the digital signal to the computer, which processes the data and then visualizes a figure based on the received information. Finally, the blue arrow indicates that the person percepts the changing visual information through the eyes which might alter the human's brain activity. The three actors form a closed-loop (feedback) control system. The figure was created with Draw.io and Photoshop, and some of the graphical elements are used under a free license provided by Vecteezy.com.

3.2 EEG prototype

3.2.1 Requirements of the EEG system

The system design of the EEG device was based on the predefined requirements, which were the following:

- Ability to perform neurofeedback
- Portable
- Simple and easy-to-use
- Customizable electrode placement
- High signal quality
- Robustness to artifacts and ambient noise
- Low-cost

Most of these initial requirements could be satisfied by selecting the appropriate hardware pieces, while the rest could be implemented in the firmware of the prototype. For example, portability, simplicity, and ease of use were achieved by utilizing a single-channel amplifier. High signal quality was ensured by the choice of the amplifier, analog-to-digital converter, and electrodes. A 3D-printed handband was designed to provide portability, customizability, and modularity, while simultaneously robustness to artifacts. Finally, PC software was implemented to ensure the ability to perform visual neurofeedback. The final system consisted of hardware components, electrodes, a headband, and supporting software, which will be discussed in the upcoming sections.

3.2.2 Hardware

The hardware components included a single-board microcontroller (Arduino Nano), an amplifier circuit (EEG Click), and electrodes. The electrodes consisted of three disposable biomedical sensor pads and a cable for three electrode endings. The essential components of the prototype can be seen in Figure 2. Besides these items, other miscellaneous items were used, such as a breadboard, some connection wires, and a USB cable for the interconnection. The hardware components will be discussed individually in the upcoming sections.

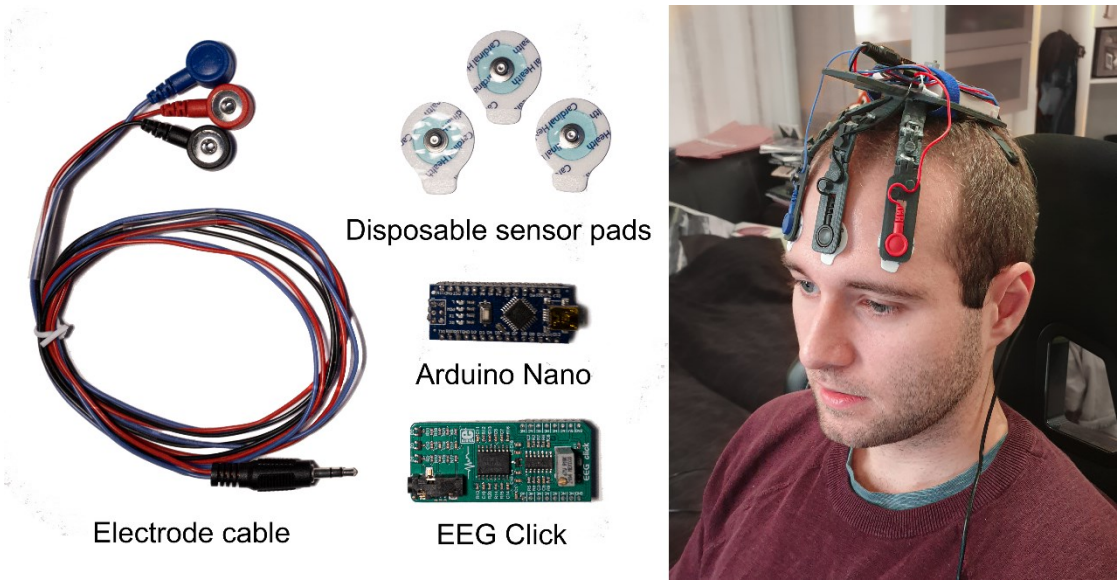

Figure 2 –The components of the proposed EEG device: Arduino Nano, EEG click, and the electrodes including a cable and three disposable sensor pads (LEFT). The assembled prototype during a physiological measurement (RIGHT).

3.2.2.1 Arduino Nano

Arduino Nano is a microcontroller development board, and it was the master of the EEG system, as it was responsible for controlling the system's functionality. Its primary purpose was to periodically read the analog value of the output of the signal amplifier at the rate of 256 Hz and to transmit the acquired data through a serial port to the PC. The developer board's most crucial component is the Atmega328p microcontroller; its most important technical parameters are listed in Table 2.

Table 2 - Technical parameters of the microcontroller [31]

Technical parameter	Value
Core clock frequency	16 MHz
Word size	8 bits
Flash memory	32 KB
EEPROM	1 KB
SRAM	2 KB
ADC resolution	10 bits
Logic voltage level	5V

These technical parameters seemed to be sufficient to meet the requirements. Regarding the project, the most critical input and output (I/O) ports were the analog input (A1) and Mini-B USB connection (serial) output.

3.2.2.2 EEG click

EEG Click is a single-channel EEG signal amplifier module designed for medical research applications. The circuit consisted of a precision instrumentation amplifier (INA114), a 4-channel op-amp IC (MCP609), a reference voltage IC to create a positive virtual ground potential (MAX6106), a potentiometer, and several discrete components, such as resistors, capacitors, and diodes [32]. The precision instrumentation amplifier had a minimum 100 dB common-mode rejection ratio, and a maximum offset voltage of 50 µV [33].

EEG Click utilizes the driven right leg (DRL) electrode placement scheme, which decreases the common-mode noise in the signal by feeding back the inverted common-mode voltage to the patient [34]. The name originated from the electrocardiography method when the patient's right leg served as the reference point. Because of this, the EEG Click supports three electrodes: the positive, the negative, and the DRL electrode, where the positive electrode is the active channel. The output is the amplified value of the differential inputs (positive and negative electrodes) minus the DRL electrode. The circuit is powered by 5 V, and it has a four-pinned 3.5 mm phone connector (also known as Jack) analog input and an analog output pin in the range of 0-5 V. The total gain of the circuit is between 780 and 7800 times, which can be adjusted by rotating the potentiometer [32].

3.2.3 Electrodes

The electrodes of the proposed EEG system consisted of a cable and three disposable biomedical sensor pads (wet electrodes). The electrode cable comprised three leads which end in a 3.5 mm audio jack connector on the common side, and three snap-style receptacles (buttons) on the other side to connect to sensor pads. The electrode pads were composed of a sensor, a connector, and an adhesive gel. The sensor was Ag/AgCl coated polymer, the connector was stainless steel, and pressure-sensitive adhesive and conductive hydrogel, while other parts were made of paper, polypropylene, and polyethylene film [35]. The electrodes had an ACZ impedance of 220 Ω and a DC offset of 0.2 mV. The prototype was used only with this kind of wet electrode.

3.2.4 Headband

The headband had a dual role as it held the hardware components together on the top of the head and significantly diminished the cable movement/sway artifacts by holding the cables firmly. The headband was custom-designed in Tinkercad (tinkercad.com), an online 3D modeling program, and the final design was printed by a Voxelab Aquila C2 3D Printer using polylactic acid (PLA) material. The headband was modular and it consisted of more than ten parts, connecting each other with one-degree-of-freedom hinge joints. The modularity made the electrode holders adjustable and customizable. The latest version of the headband had five fixed electrode positions: AF7, Fpz, AF8, TP9, and TP10, based on the international 10-10 electrode system (IS 10-10). In the default configuration, AF7 was the positive electrode, AF8 was the negative electrode, and FPz was the DRL electrode (TP9 and TP10 were unused). Figure 3 shows the part of the headband in computer-aided design (CAD) view.

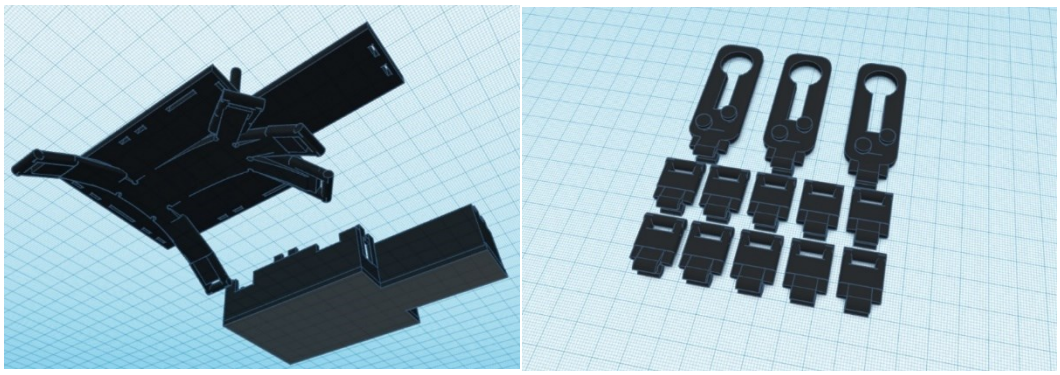

Figure 3 - Parts of the headband in CAD view. The LEFT image shows the main headband piece (lefthand side), and the cover box (righthand side). The RIGHT picture shows the pieces of the modular electrode cable holders. The screenshots were taken from Tinkercad.

3.2.5 Software

During the project, three pieces of standalone software were developed: the firmware for the embedded device, a computer application for real-time data recording (and optional plotting), and a computer application for real-time visual neurofeedback training.

3.2.5.1 The firmware

The firmware was the embedded software that ran on the Arduino Nano while powered. The firmware was implemented in C language using the Arduino Studio SDK environment, and it had two main functions:

- Data acquisition from the analog output of the amplifier
- Data transmission to the PC via serial port

The analog data acquisition was implemented by timer interrupts to ensure coherent sampling at the rate of 256 Hz. In order to do this, the analog-to-digital converter (ADC) was using auto trigger mode based on a hardware timer interrupt. The choice of timer delay (sample rate) and window length is crucial for coherent sampling. Should the sampling not be coherent, it would result in spectral leakage and might ruin further EEG applications.

The data was transmitted on the serial port (USB) at BAUD of 500 000. The ADC had a resolution of 10 bits; thus, the newly acquired digital value was stored in an integer. After converting it to a string, the value was transmitted on the serial port characters by characters (ASCII) once it was ready.

3.2.5.2 Real-time data recording application

This application was designed to record the output of EEG devices in real-time (online) and store them on a PC. The program was meant to run on Windows 10 operating system with multiple CPU cores. This application supported the prototype and a commercial device. The program was written in Python language, and it utilized multiprocessing. The program had three main functions:

- Reading periodically the output of the target EEG system
- Writing periodically the output,
- Displaying and updating periodically animations, graphs, or other visual information (optional)

For these three functions, three separate processes were implemented. One process periodically read the input as soon as new data arrived, roughly at every 3.9 ms. In the case of the custom device, the data were directly read from the serial port. In the commercial EEG device's case, however, third-party software was also used, called BlueMuse, which acted as middleware for streaming the data through the lab streaming layer (LSL) [36]. The process read the EEG voltage values from the selected LSL channels, then stored these values in a buffer, and once the buffer was full, the process passed the buffer's content to a queue so that the second process could access the buffered data with this interprocess communication.

The second process took the buffered chunk of data out of the queue, pre-processed them such as converting the raw unsigned integer values to real numbers, or applying some digital filtering with an FIR filter if necessary. By default, only an anti-alias filter was applied, a low-pass filter with a cutoff frequency of 127 Hz. Finally, the process wrote the pre-processed data to the selected output file. The default output file type was .txt and stored data were separated by commas and whitespaces.

The third process could display visual information, such as animation on the screen, which was essential for specific EEG measurements. This process ran simultaneously with the first data acquisition process. The third process also could plot the raw time domain signal and amplitude spectrum of the last 1 second of received data in "real-time". The update frequency could be altered; its default value was 16 Hz. This third process was optional; it could be toggled on or off.

3.2.5.3 Real-time neurofeedback (demo) application

This application was designed to demonstrate the neurofeedback capabilities of EEG devices. It was compatible with the prototype and a commercial device. The demo application simulated a roller coaster ride with real-time neurofeedback, where a point-of-view (POV) video of the first passenger seat was replayed on the screen. The replay speed (the frames per scond rate) was dependent on the feedback value. The physiological input of the transformed feedback was the mean PSD of the theta band. The whole neurofeedback exercise lasted for roughly 3 minutes. The first 90 seconds was the baseline recording phase, while the rest was the actual neurofeedback session, whose exact length depended on the frame rate. The program was written in Python language, and it utilized multiprocessing. It was meant to run on Windows 10 operating system with multiple CPU cores, and its average response time was under 100 ms. This neurofeedback application was based on the recording application, as they shared some functionalities. The application had three main functions:

- Reading periodically the output of the target EEG system
- Buffering and pre-processing the acquired data, calculating the feedback value
- Replaying a video at changing frame rate based on the feedback value.

These three different functions were implemented by three separate processes that ran individually; however, they communicated with each other with queues. One process periodically read the output of the target EEG system as soon as new data arrived. The reading was synchronized to the EEG system; therefore, data were sampled at 256 Hz. The data was directly acquired from the prototype case's serial port (USB). In the commercial EEG device's case, however, third-party software was also used, called BlueMuse, which acted as middleware for streaming the data through the LSL [36]. The process read the EEG voltage values from the selected LSL channels. The acquired data was buffered, and once the buffer was full, the process passed the buffer's content to the first interprocess queue so that the second process could access the raw data.

The second process took the buffered chunk of data out of the first queue. By default, only an anti-alias filter was applied to the acquired data, a low-pass filter with a cutoff frequency of 127 Hz. Power spectrum density was calculated from the last 256 acquired samples, then the PSD values of the frequency range of interest were averaged. By default, the theta band (4-8 Hz) was chosen for this frequency range. During the baseline recording phase, the dynamic range was determined by measuring the minimum and maximum values of the PSD. During neurofeedback, however, the mean PSD value was one of the inputs of the calculated feedback. More precisely, the algorithm calculated the new feedback value based on the dynamic range, the current PSD value, and the last feedback value. In the end, the feedback value determined the frame rate of the replayed video. Therefore, the second process passed the feedback value to the second queue so that the third process could access it.

The third process was responsible for displaying the neurofeedback, and it replayed the input video at a changing frame rate depending on the received feedback value. This feature was implemented with the OpenCV library. The results of several measurements showed that the highest stable frame rate was 70 frames per second (FPS), which could keep up with this realization. The standard frame rate was chosen as 30 FPS, the default value for the baseline recording. The lowest FPS value and intermediate values were calculated to form a geometric series with previous numbers when the length of the geometric series was 15. Therefore, the maximum FPS value was 70, while the minimum was 12.8. The FPS of the video was proportional to the feedback value during positive, while inversely proportional to the feedback value during negative feedback setting. The default setting was negative feedback; in other words, there was a "brake" in the system. For example, when the replay speed was too fast, it might have stimulated increased alertness in the brain, which was translated to a small feedback value and thus resulted in a low FPS rate, slowing the video down. The displayed video was downloaded from YouTube [37]. Three screenshots were taken from various parts of a neurofeedback session; they can be seen in Figure 4.

Figure 4 - Screenshots of the neurofeedback applications at various frame rates. The current FPS can be seen in the top left corner in green. Baseline recording at normal FPS (TOP); neurofeedback at high FPS (MIDDLE) and low FPS (BOTTOM). The screenshots were taken from the application in-flight, and the NFB is based on a video downloaded from YouTube [37].

Chapter 4

4 Materials and methods

4.1 Resources

The project was carried out in the Marianne Bernadotte Center (MBC), part of Karolinska Institutet's Department of Clinical Neuroscience. The research center's main research areas are ophthalmology, pediatric ophthalmology, eye-tracking, optometry, and visual perception [38]. Several of their studies are based on treating motion sickness. In addition, the MBC was interested in developing the previously described custom research tool for investigation and rehabilitation. MBC provided most of the required resources for the project. Kista Mentorspace, which is hosted by the KTH Royal Institute of Technology, provided all the other resources, such as lab-grade instruments and tools.

4.2 Device comparison

The scientific purpose of the thesis was to investigate the design process of a low-cost, portable, single-channel EEG system that could be used for neurofeedback applications in homecare. Besides validation, a device comparison was intended to explore the usability requirements of such a system. Therefore, the research framework included technical measurements determining the signal quality of the devices. Furthermore, four physiological measurements were performed on six human test subjects to investigate neurophysiological changes and the effect of artifacts on the EEG systems. Following practices from consumer-grade EEG comparison studies, the hypothesis was if the prototype had similar technical qualities as the commercial device then the prototype was deemed to be validated [7]. For this end, a suitable consumer EEG device had to be selected that had been validated beforehand. This upcoming synopsis introduces three candidates for this comparison, three popular consumer-grade portable EEG devices on the market. OpenBCI's Ganglion Board, NeuroSky's Mindwave Mobile 2, and InteraXon's MUSE 2 brain sensing headband were chosen for the overview. They all feature four or fewer active channel electrodes and support wireless data transfer. It is noteworthy to clarify that neither is medical grade; however, they are all scientifically-tested research tools for various applications [39] [40] [41]. Most of these devices come with dedicated software packages to record, analyze and visualize the results of EEG recordings.

OpenBCI’s Ganglion Board

OpenBCI is an open-source brain-computer interface platform designed for neuroscience and biosensing applications [42]. It started as a Kickstarter project, and the mission of the company was "[...] to lower the barrier to entry for brain-computer interfacing while ensuring that these technologies are adopted into the consumer landscape in an ethical way that protects user agency and mental health" [42]. OpenBCI does not refer to a single device but a wide selection of hardware modules, the different versions depending on the target application. For this overview, the cheapest

and simplest board was chosen, the Ganglion Board, which costs $499.00 [43]. The Ganglion Board has four active channels, one reference, and one driven-ground electrode. The electrode positions are meant to be customizable and entirely dependent on the electrode system utilized. By default, the device has a sampling rate of 200 Hz, and its ADC has a resolution of 24 bits. The device communicates with Bluetooth Low Energy by default, but it can be extended with Bluetooth Classic and Wifi modules to increase throughput and range.

InteraXon's MUSE 2

InteraXon's MUSE 2 brain sensing headband (Muse) was designed to become a meditative device, performing biofeedback applications to relax, meditate, and improve sleep [44]. It is a headband device with seven dry EEG electrodes, which comply with the international 10-10 electrode system: AF7, AF8, TP9, and TP10 electrodes are the active channels, Fpz is the DRL electrode, while Fp1 and Fp2 (interconnected) are the CMM electrodes. Muse's EEG has a sample rate of 256 Hz, and its ADC resolution is 12 bits. Besides the EEG sensors, the headband also features photoplethysmogram (PPG), pulse oximetry, accelerometer, and gyroscope [44]. The device streams the data via Bluetooth. Muse is available in most countries, and its retail price was €269.99 (at the time of access to the manufacturer's website).

NeuroSky's Mindwave Mobile 2

Mindwave Mobile 2 (Mindwave) is a single-channel, wireless, headset EEG device that is meant to be used for meditation, research, education, and entertainment purposes [45]. The device comes with prebuilt algorithms that can measure attention, mediation, and mental effort. Even there are natively supported tools to detect eye blinks. Mindwave has only three electrodes; its active channel electrode is in the Fp1 position, while the ground and reference electrodes are in A1 and T4 positions, respectively [45]. Its ADC resolution is 12 bits, and the device's sample rate is 512 Hz, yet Mindwave can only record in the 3-100 Hz frequency range. The device is wireless, and it supports both Bluetooth Classic and BLE. The MindWave Mobile 2: Brainwave Starter Kit costs $109.99. A comparison of the previously introduced three EEG devices and the in-lab prototype can be seen in Table 3.

Table 3 - Comparison of the EEG devices [43] [44] [45]

Device	Electrodes		Electrode placement	Sample rate	ADC resolution	Price
	Active (channel)	Indifferent (REF/GND/DRL)				
Ganglion Board	4	2	Customizable	200 Hz	24 bits	€455.0*
Muse	4	3	Fixed	256 Hz	12 bits	€269.9
Mindwave	1	2	Fixed	512 Hz	12 bits	€100.0*
Prototype	1	2	Customizable	256 Hz	10 bits	€85.0**

*Original price ($) was converted to €, then rounded up.

**Estimate of the hardware costs, which does not include the 3D-printing costs. This material cost is in contrast with retail prices of the other three devices.

Ultimately, Muse was chosen for the device comparison, partially because Muse was previously validated by the research group for rehabilitation and neurofeedback applications [46]. In addition, several other studies showed promising results that Muse was an easy-to-use and viable research tool for ERP research, spectral analysis, and BMI application for robot control. [41] [47] [48]. Moreover, Muse's qualities were the most appealing of the three commercial devices in the introduction all things considered. The device is relatively inexpensive, yet it offers some flexibility with the choice of channel electrodes and can provide stable, high-rate wireless communication without data compression. Lastly, the availability and accessibility of the device within the research group were also in huge favor of this choice.

4.3 Configuration

An important aspect of the project was to investigate the effects of artifacts on the EEG devices. Artifacts are much like noise; they are unwanted elements in the signal that may corrupt the otherwise clean data of the EEG recordings. Generally, two major types of artifacts can be distinguished in the field of EEG: physical (technical) and physiological (non-technical/biological). However, some academic publications break down the technical one into two categories based on its source: acquisition system-based artifacts and electrical interference and external equipment-based artifacts [6]. The most notable physical artifacts include the power line noise, the cable sway and electrode displacement, and the internal noise of the EEG system. On the other hand, the origin of the physiological artifacts is the human body's biological processes, except for the neural activities that are the study of interest. Biological artifacts include muscle movements, such as head and neck movement, ocular (eye) movement, electrocardiographic, perspiration, and respiratory activities [6].

As stated earlier, the active channel of the prototype was the AF7 electrode. For simplicity and compatibility reasons, Muse’s one active channel, the AF7 electrode, was recorded only during the measurements; the other three active channels were not recorded. Eye movement artifacts can primarily be detected in the frontal lobes and the magnitude of the artifact is based on the closeness of the electrode to the eyes [6]. Since the AF7 electrode was used for both devices as an active channel, examining the eye movement artifact was recommended. Besides eye movement, movement-induced artifacts were deemed relevant for the application of the devices. In the end, the artifacts of interest to be examined were eye movement, muscle movements such as head and neck movement, cable sway, and electrode displacement. They were identified as primary artifacts which could significantly corrupt the signals yet could be easily detected. The effect of these artifacts was investigated during the physiological measurements conducted on test subjects. There was no dedicated measurement for the effect of the powerline noise. Instead, all measurements were influenced by the 50 Hz alternating current (AC) noise because neither was conducted in an electrically isolated room, but rather in rooms where the density of electric appliances was high. This also meant the effect of switching ON and OFF artifacts could be observed in the recordings. During the offline data analysis, the AC power noise was filtered out with a rather narrow infinite impulse response (IIR) notch filter, where the middle of the band stop frequency was 50 Hz, and the filter's quality factor was 35. The online recording software also included an optional notch filter; however, it was turned off.

The two EEG devices were measured purely by technical measurements to determine signal quality and physiological tests to reveal changed brain activity and induce artifacts. Later the same tests were performed on the other device and concluded the validation process. For this end, the

custom recording software was used as both devices were compatible with the computer applications mentioned in 3.2.5.2 and 3.2.5.3. Prior to the measurements, the recording computer software was validated and verified. In Muse's case, the output of the custom software was compared to the output of third-party software, Mind Monitor. In the prototype cases, the recording software's output was compared to the raw digital values of the system produced by EEG Click and the microcontroller's firmware. The output was in the expected value range, the numbers aligned with the recording, and no data was lost. Besides these data comparisons, unit tests were done on the software to ensure quality and functionality.

4.4 Technical measurements

The purely technical measurements aimed to determine the signal quality and amplitude-frequency characteristics. As the first step, an artificial scalp system was created, with two pieces of metal sheets representing two different areas of the human scalp. The system also generated electrical signals, simulating those that an EEG may record. Therefore, this artificial scalp served a dual role: it generated clean sinusoid signals in the neural oscillation frequency and voltage level and provided a physical interface for both devices: a convex curved metal sheet for Muse and stick-on disposable electrode pads for the prototype. One scalp was meant for the positive (active) electrode, and the other was for the negative and DRL electrodes. The electric signals were synthesized by a Hewlett Packard 33120A model precision function generator, and its output had a minimum amplitude of 50 mV. Since the EEG voltage levels are in the hundreds of microvolts range, the output of the function generator had to be scaled down with a resistive voltage divider, which was realized with two resistors (R1 and R2). The values of R1 and R2 were chosen as 2.68 kΩ and 12 Ω, respectively, because the divider would scale down the 50mV signal into 225µV with these resistance values. A schematic diagram of the artificial brain can be seen in Figure 5.

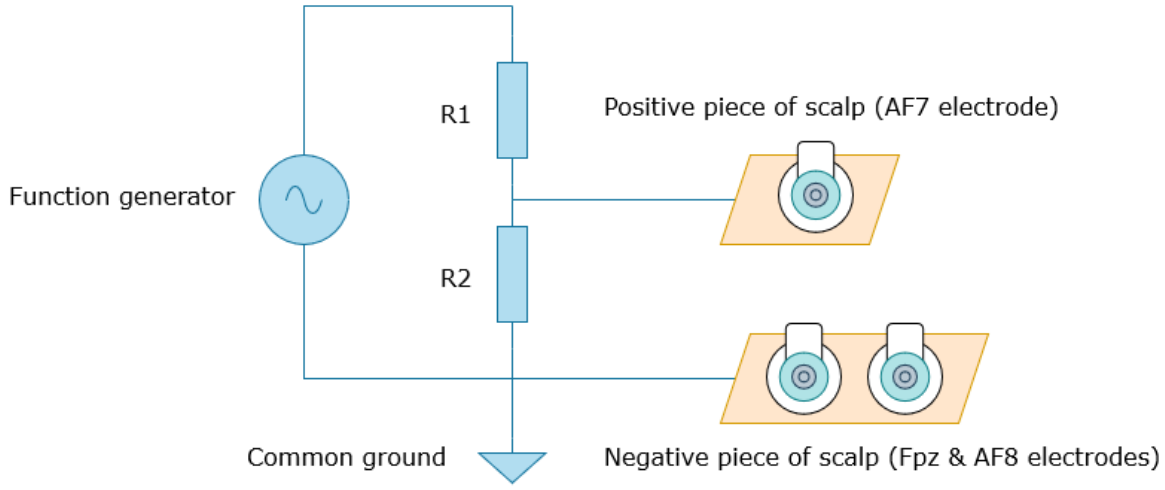

Figure 5 - Schematic diagram of the artificial scalp. It consists of a functional generator, a resistive voltage divider, and two copper plates (with one and two electrode pads). The figure was created with Draw.io.

Before usage, the voltage divider had to be validated. As the first step, the impedance of each discrete component was measured by a Philips PM 6303A automatic RCL meter. Table 4 contains the

measured impedance of the components. The positive scalp contained the R1 resistor with a relatively high impedance. Moreover, each electrode pad added roughly 200 Ω to the system, but this only affected the measurements that belonged to the prototype. This extra added impedance might have reduced the signal-to-noise ratio; however, it was not expected to influence the methodological approach to any significant degree.

Table 4 - Measured impedance of the components

Component	Absolute impedance | Z |	Phase angle (φ)
R1	2.679 kΩ	0.0 °
R2	12.02 Ω	0.0 °
Positive scalp	2.68 kΩ	0.0 °
Positive scalp with an electrode pad	2.877 kΩ	-0.2 °
Negative scalp	0.191 Ω	0.4 °
Negative scalp with two electrode pads	137.1 Ω	-1.7 °

The next step of the validation was determining the voltage divider's divide-down ratio and measuring the system's output. The nominal values were calculated based on the values of components, while the actual voltage levels were measured by a Hewlett Packard 34401A Digital Multimeter (DMM). An input signal of 1 V peak value was chosen for measurement, equal to 0.707 V root-mean-square (RMS). The divide-down ratios were calculated as the outputs were divided by the respective inputs. The results can be seen in Table 5.

Table 5 - Voltage divider parameters

Case	Input (RMS)	Output (RMS)	Divide-down ratio
Nominal	0.707 V	3.152 mV	0.0045
Measured	0.689 V	3.085 mV	0.0045

The measured divide-down ratio was equal to the nominal one, and the voltage divider was assumed to work as intended. All the upcoming technical measurements were performed using this artificial scalp. The gathered data were processed, analyzed, and visualized in MATLAB R2021b.

4.4.1 Amplitude-frequency characteristics

The purpose of the assessment was to determine the amplitude–frequency characteristics (more precisely, frequency-limited, real value transfer (amplitude) characteristics). The frequency band of interest was chosen as 3-60 Hz, covering the whole theta-alpha-beta band and a significant part of the gamma wave range. Frequencies outside of this range were deemed irrelevant and, therefore, were not calculated. Consequently, the measurement frequencies were chosen as 3, 6, 9, 12, 15, 20, 30, 40, 50, and 60 Hz. As was stated earlier, the amplitude of the sinusoids was originally 50 mV, which was scaled down to 225 µV. With the recording software introduced earlier, unfiltered data was directly acquired with 1 second of time windows. Later these raw, time domain data were imported into MATLAB, and an IIR anti-aliasing filter was applied to them, then the amplitude spectrum was calculated by performing FFT on each data set. Next, the ten spectra of each device were merged to form a single aggregated diagram (bar chart), where the DC component was removed, therefore only containing the highest amplitude component of each original spectrum. As a final step, a 5th-order

polynomial curve was fit on the frequency bars indicating the form of the "transfer characteristics" of the system. Both frequency (x) and amplitude (y) axes were chosen as linear scales instead of the logarithmic scale of the Bode plot because the linear scale would show differences more clearly in these limited ranges.

4.4.2 Signal quality

This measurement aimed to determine the signal quality of the devices. The input signals of these measurements were the ten clean sinusoid signals (3-60 Hz) introduced in the previous section. For this end, four quantitative measures were chosen:

- Signal-to-noise ratio
- Signal-to-noise and distortion ratio
- Spurious-free dynamic range
- Total harmonic distortion.

The signal-to-noise ratio (SNR) is the most elementary signal quality metric, but the actual definition may vary. In most cases, SNR refers to the ratio of the root-mean-square value of the fundamental signal (clean sinusoid) to the mean value of the root-sum-square (RSS) rest of the components, where harmonics and DC component is excluded [49]. SNR was calculated with MATLAB function *snr()*, excluding the power of the first five harmonics. The output was relative to the carrier in decibels (dBc). The signal-to-noise and distortion ratio (SINAD) is like SNR, but all harmonics are included in the calculation, while the DC component is excluded [49]. SNR was calculated with MATLAB function *sinad()*. The output was relative to the carrier in decibels (dBc). Spurious-free dynamic range (SFDR) refers to the ratio of the fundamental signal's RMS to the most dominant spurious RMS [49]. SFDR was calculated with MATLAB function *sfdr()*, and the DC component was excluded. The output was in decibels (dB). Total harmonic distortion (THD) refers to the ratio of the RMS value of the first harmonic to the mean value of the RSS of its harmonics [49]. THD was calculated for the first five harmonics with MATLAB function *thd()*, and the output was in decibels (dB).

4.5 Physiological tests

The purpose of the physiological tests was to show the altered brain activities of humans and to reveal potential artifacts for various stimuli. Both can be directly observed through changes in the recorded spectrum, so frequency domain analysis, more specifically power spectral density, was the primary investigating tool. These measurements were done on Muse, and the prototype with the same conditions applied, and the recordings took place shortly after each other, which ensured similar mental conditions. The tests were conducted on six human subjects: four males and two females, aged between 21-31 (mean: 26.0, std: 3.11).

There was a total of four physiological measurements: inhaling and exhaling (breathing) exercise, head and neck movement exercise, eye movement exercise, and paced auditory serial addition test (PASAT). The measurements were recorded with the software mentioned in 3.2.5.2. During the recordings, for each measurement, the respective animation was displayed by the software. The only exception was PASAT, where an audio file was played instead.

The recordings contained an epoch for each stimulus, and each epoch lasted for a minute. The first epoch was the baseline in every recording, and it served as a reference for the other sub-measurements. Brain activity changes were evaluated based on the (mean PSD) difference between the baseline and epoch containing the stimulus. After the recordings, the data was imported into

MATLAB for processing and analysis. Later the 60-second-long epochs were reduced to 20 seconds by manually selecting a continuous subset of the original epochs. This aimed to eliminate transients and remove recording errors, such as peaking signals, which would corrupt the spectrum. If the epochs of the recordings could not have been cleaned from such errors, they would be discarded completely. However, this rejection of recordings was bilateral; if a subject's Muse recording was corrupted and therefore rejected, their custom device recording was also discarded, regardless of its quality. This consequence ensured fidelity in the comparability as it allowed for within-subject comparisons for all participants. The new 20-second-long epochs would still include the changed fundamental brain activities as well as technical and physiological artifacts while retaining similar variance in the signal. Later the separated epochs were contaminated and then filtered. An IIR lowpass filter with a cutoff frequency of 60 Hz, an IIR high pass filter with a cutoff frequency of 0.5 Hz, and an IIR notch filter with a cutoff frequency of 50 Hz were applied to signals. The theta, alpha and beta bands were selected as relevant brainwaves for the study, and their frequency ranges were defined as 4-8 Hz, 8-12 Hz, and 12-30 Hz respectively. The PSD values were converted to decibels (dB), then they were averaged for each frequency bin in the given brain wave (frequency range), e.g., alpha activity was calculated by taking the means of PSD values between 8 and 12 Hz. This resulted in three values for each device for each epoch. These values were used for the input of statistical analysis.

After the filtering, power spectral density was calculated for each epoch using a rectangular window with the *periodogram()* MATLAB command. Other kinds of windowing, such as Hann or Hamming, were not considered as they would distort the natural spectra of interest. The theta, alpha, and beta bands were selected as relevant brainwaves for the study, and their frequency ranges were defined as 4-8 Hz, 8-12 Hz, and 12-30 Hz, respectively. Consequently, the delta and gamma bands were excluded as they were out of the frequency range. The outputs of the periodogram, the PSD values were converted to decibels, and then they were averaged for each frequency bin in the given brainwave frequency range. E.g., alpha band activity was calculated by taking the mean values of PSD between 8 and 12 Hz. Since only theta, alpha, and beta bands were meant, this resulted in three values for each device for each epoch.

MATLAB's output was used for the input of statistical analysis, which was done in IBM SPSS Statistics 26 for the four measurements. The first step for all cases was to perform the Shapiro-Wilk test that revealed whether the measurements, categorized by frequency ranges: theta, alpha, and beta bands, were normally distributed or not. Then repeated measures analysis of variance (ANOVA) was applied to the frequency ranges individually. For each frequency band, the main effects were calculated for the devices and the stimuli. Furthermore, the interaction effects between them were also calculated. In some cases, paired T-tests were also calculated to perform contrast tests and reveal hidden relationships. F-value with the degree of freedom and p-values were chosen to be reported in the results. The significance level for p-value, the value of alpha, was 0.05 as the convention. The following section describes each of the four major measurements in more detail.

4.5.1 Breathing exercise

The EEG devices were tested to detect electrophysiological biomarkers of altered levels of alertness in the form of specific brainwave frequency power. The hypothesis was that the lower level of alertness was associated with an increased power spectrum of theta and alpha frequencies. The brainwaves collected in the experiment were in the theta, alpha, and beta bands. Levels of alertness were measured with a controlled breathing pattern. This measurement aimed to reveal the differences in neural activity between breathing heavily and breathing lightly. Typically, it is easier to start at a high breathing rate than reach a low breathing rate. Because of this consideration, the measurement started at a relatively high rate of 20 breathing cycles (inhaling and exhaling) per minute, which served as the baseline, then the breathing rate gradually decreased. Once it reached the lowest value, 4 breathing cycles/minute, it increased to 20 cycles per minute. The exact sequence of changing

breathing rate was 20 (baseline), 15, 12, 10, 8, 6, 5, 4, 12, and 20 breathing cycles per minute. This exercise was expected to be physically challenging to perform. Therefore, there were intermediate breathing rates to smoothen the transitions, especially between high and low breathing rates. Each breathing cycle was split into 40% inhaling and 60% exhaling time. For example, the 20 breathing cycles per minute indicated that a breathing cycle was 3 seconds long, of which the inhaling phase was 1.2 seconds, while the exhaling phase was 1.8 seconds. Everyone performed the breathing test in the same sequence, wearing first the prototype and, subsequently, the Muse headset. There was a looming ball animation on the computer's screen to synchronize the breathing rate, which ran in parallel with the recording. The frame rate of the animation was roughly 30 FPS. In the animation, the ball gradually got bigger and brighter as it approached the end during the inhaling phase, and it got smaller and darker as it went toward the end during the exhaling phase. Every cycle lasted for a minute which was in line with the epoch length. A sequence of the exhaling animation can be seen in Figure 6.

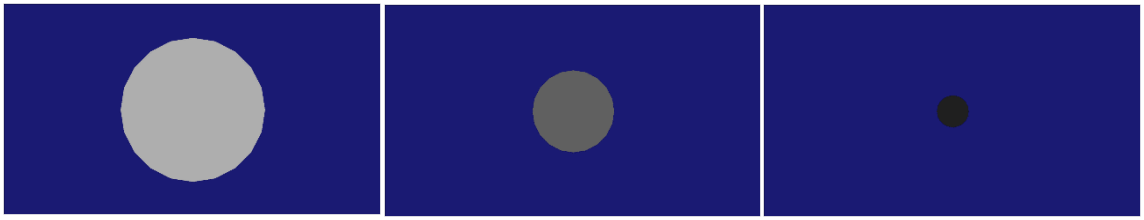

Figure 6 – Screenshot sequence of the exhaling animation from the breathing exercise. From LEFT to RIGHT, the looming ball gets smaller and darker as it reaches the end of the exhaling phase. The screenshots were taken from the custom data recorder application.

4.5.2 Eye movement exercise

The EEG systems were tested to detect electrophysiological biomarkers of eye movement artifacts in the form of specific brainwave frequency power. The statistical approach for this analysis was data-driven, given no a priori hypothesis on which brainwave frequency range was typically associated with eye-movement artifacts during EEG recordings. The brainwaves collected in the experiment were in the theta, alpha, and beta bands. There were three sub-measurements of interest besides the baseline; thus, there were four epochs in total: baseline, eyes closed, horizontal (lateral) eye movement, and circular (rotational) eye movement. Each sub-measurement lasted for a minute. During the recording, the test subjects were instructed to stay still; move, and blink as little as they could, especially during the first two epochs. Various animations were replayed on the computer's screen to synchronize the eye movement, which ran in parallel with the recording. Each individual performed the eye movement in the same sequence, wearing at first the custom headset and subsequently the Muse headset. The sub-measurement in more detail:

Baseline: The test subjects were asked to focus on a small static red dot in the center of the screen.

Eyes closed: The test subjects were instructed to close their eyes. The screen was completely black during this time, and no animation was replayed.

Horizontal eye movement: The test subjects were asked to follow the red dot on the screen with their eyes, which altered between a left-side and a right-side position for 2 seconds.

Circular eye movement: The test subjects were asked to follow the red dot on the screen with their eyes, circulated clockwise around a point in the middle of the screen. The period of circulation was approximately 2.75 seconds. Figure 7 shows four screenshots of the animations for each sub-measurement.

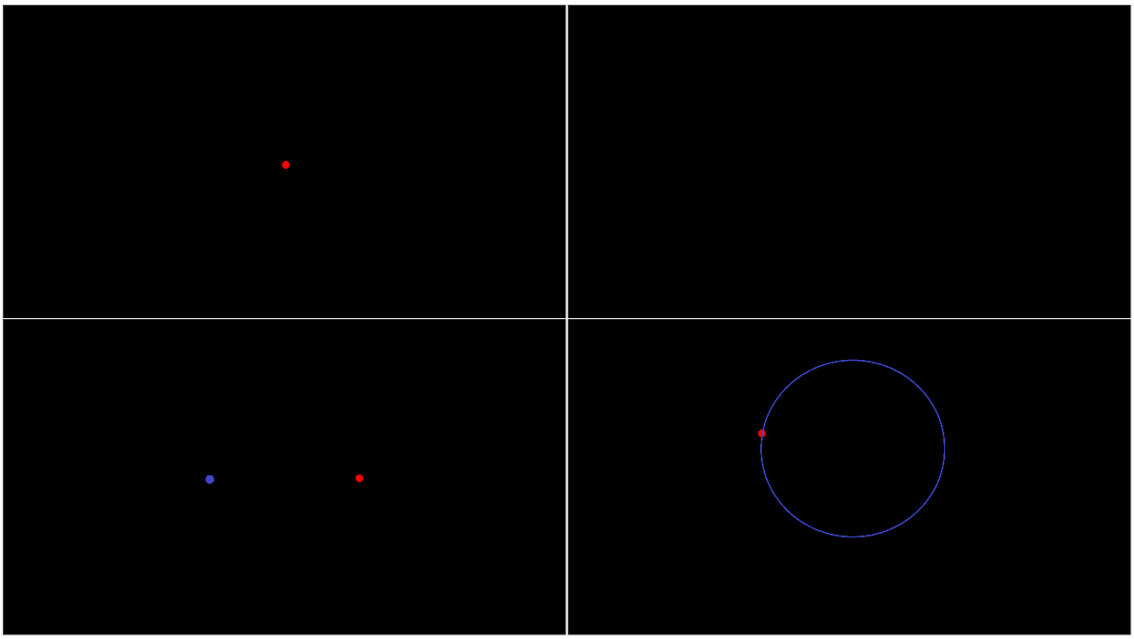

Figure 7 – Screenshots of the eye movement animations. The figure shows the baseline (TOP LEFT), closed eyes (TOP RIGHT), horizontal eye movement (BOTTOM LEFT), and clockwise circular eye movement (BOTTOM RIGHT). The red color indicates the original animation, while the blue color helps to illustrate the motion of the animation for the last two sub-measurements, and it was not present during the recording. The screenshots were taken from the custom data recorder application.

4.5.3 Head movement exercise

The EEG devices were tested to detect electrophysiological biomarkers of head movement-related artifacts in the form of specific brainwave frequency power. The purpose of this test was to reveal muscle movement-based physiological artifacts, as well as technical artifacts such as cable sway and electrode displacement. The measurement would also unveil which rotation axis was the most dominant regarding these artifacts. The statistical approach for this analysis is data-driven, given no a priori hypothesis on which brainwave frequency range is typically associated with head movement artifacts during EEG recordings. The brainwaves collected in the experiment were in the theta, alpha, and beta bands. There were three sub-measurements, thus four epochs in total: baseline, head movement along the yaw, pitch, and roll rotational axes. The rotation axis alignment followed the general convention; the reference can be seen in Figure 8.

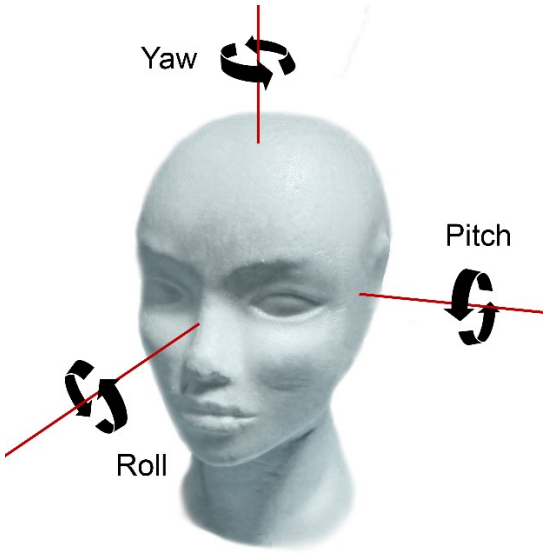

Figure 8 - Reference for the rotation axes used for the head movement recording. The figure was created in Photoshop.

Everyone performed the head movement test in the same sequence, wearing at first the prototype and subsequently the Muse headset. During the recording, test subjects were asked to sit still, move only the parts they were instructed to move, and blink as little as they could. Various animations were replayed on the computer's screen to synchronize the head movement, which ran in parallel with the recording. Figure 9 shows screenshots of the animations for each sub-measurement.

Baseline: The test subjects were asked to focus on a static red dot in the center of the screen (black background). They were instructed to sit still and not to move their heads.

Yaw axis rotation: The test subjects were asked to rotate their heads along the yaw axis following a red dot with a trajectory on the screen and synchronize their movement to the dot's movement. The rotation angle (end-to-end) was approximately 150 degrees, and the period was roughly 2.7 s.

Pitch axis rotation: The test subjects were asked to rotate their heads along the pitch axis (vertically) following a red dot with a trajectory on the screen. The rotation angle (end-to-end) was about 60 degrees, and the period was roughly 2 s.

Roll axis rotation: The test subjects were asked to rotate their head along the roll axis following a red dot with a trajectory on the screen. The rotation angle (end-to-end) was roughly 75 degrees, and the period was roughly 4.7 s.

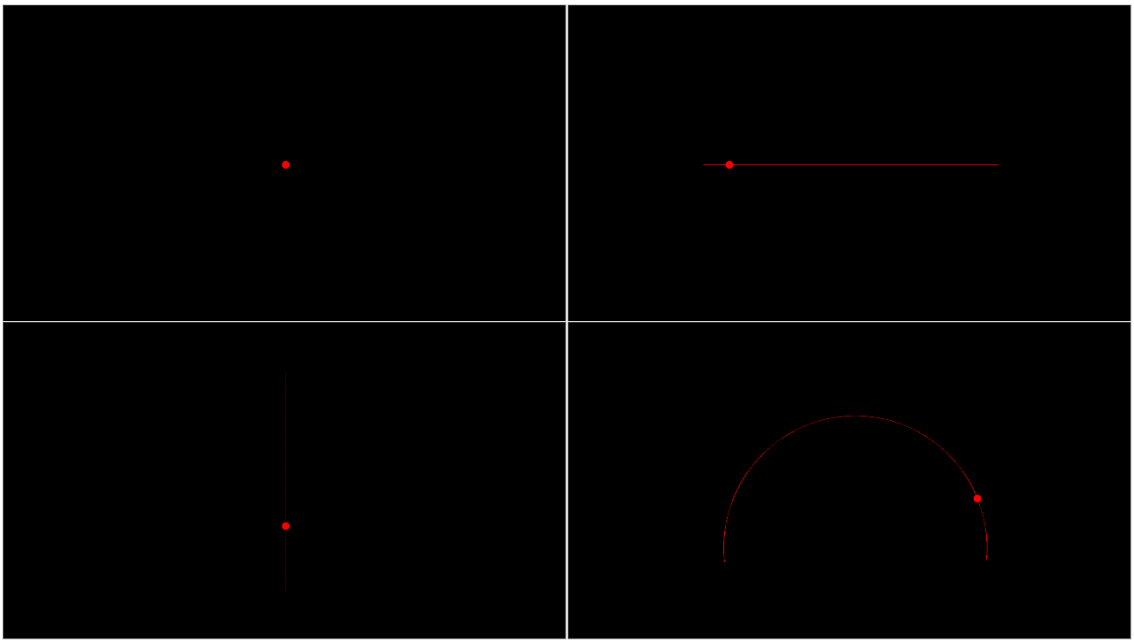

Figure 9 – Screenshots of the head movement animations. The figure shows the baseline (TOP LEFT), yaw axis rotation (TOP RIGHT), pitch axis rotation (BOTTOM LEFT), and roll axis rotation (BOTTOM RIGHT). The screenshots were taken from the custom data recorder application.

4.5.4 Paced auditory serial addition test

Paced auditory serial addition test (PASAT) is a commonly used neuropsychological test to assess various cognitive functions mainly related to attention and information processing [50]. It was originally designed to evaluate the effects of traumatic brain injuries on cognitive functioning. In a more general sense, PASAT can refer to visual and auditory stimuli. In this study, however, it exclusively means auditory stimuli. PASAT can be a reliable test under specific clinical conditions. Usually, a score is assigned to the patient's performance after the test, and the results are evaluated in contrast to the available normative data [50].

In this study, PASAT was only a stimulus to induce complex brain functioning in the prefrontal cortex area. Therefore, scores were not kept nor evaluated during the test. Instead, the EEG devices were assessed to detect electrophysiological biomarkers of attention and other cognitive functioning in the form of specific brainwave frequency power. The statistical approach for this analysis was data-driven, given there was no priori hypothesis on which brainwave band was typically associated with PASAT stimulus during EEG recordings. The concept of the experiment was simple: test subjects listened to an audio file, where numbers were told at an interval of 2.5 seconds. The test subjects periodically needed to add up the currently heard and last numbers and pronounce the results. The replayed audio file was 1 minute long, recorded within the MBC beforehand, and created for a paced auditory serial addition test for a different study. The brainwaves collected in the experiment were in the theta, alpha, and beta bands. The measurement consisted of two epochs: the baseline and the actual paced auditory serial addition test.

Baseline: Test subjects were asked to focus on a static red dot in the center of the screen. They were instructed to move and blink as little as they could.

PASAT: Test subjects were asked to listen to a minute of a PASAT recording and say the results out loud. New numbers were told at an interval of 2.5 seconds.

Chapter 5

5 Results

5.1 Technical measurements

The purpose of the technical tests was to acquire raw data with the EEG devices and determine their signal quality. In more detail, the first test measured the frequency response of the EEG systems by approximating their amplitude-frequency characteristics in the 3-60 Hz frequency range, while the second test determined the average signal quality metrics of the input signal, such as SNR, SINAD, SFDR, and THD.

5.1.1 Amplitude-frequency characteristics

As was stated earlier in 4.4.1, 1-second-long (256 samples at 256 Hz sampling frequency) sinusoidal signals of various frequencies were recorded with Muse and the prototype utilizing the custom EEG recorder software. The signal was synthesized by the artificial scalp, and the amplitude of the signals was originally 50 mV which was scaled down to 225 µV. After the recordings, time domain signals were Fourier transformed with the FFT algorithm in MATLAB to get their amplitude spectra. The dominant frequency bin (first harmonic) was taken for each input signal and summarized in a single aggregated plot. The approximate amplitude-frequency characteristics of both devices can simultaneously be seen in Figure 10.

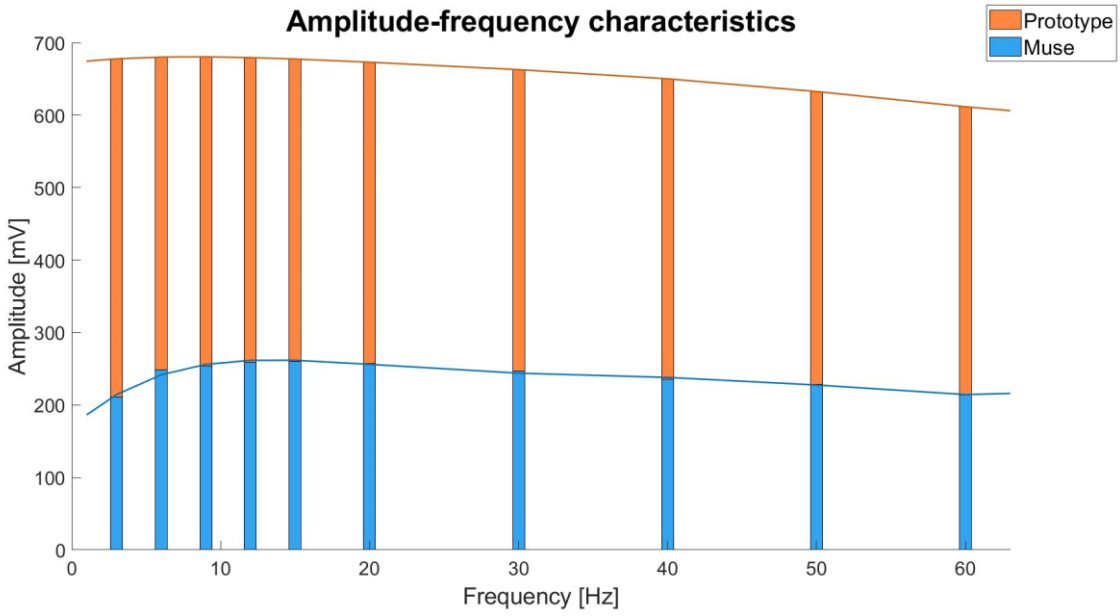

Figure 10 - Approximate amplitude-frequency characteristics of the devices. The dominant frequency bin (first harmonic) of each spectrum was taken and summarized in a single aggregated plot. The curves indicate the fifth-order polynomial which was fit to the bins and approximate the amplitude-frequency characteristics of the devices in the 3-60 Hz frequency range. The orange denotes the prototype, while the blue denotes Muse. The figure was created in MATLAB.

5.1.2 Signal quality

In order to determine signal quality, the previously introduced ten sinusoid signals were used as input to calculate the average signal quality metrics in MATLAB. In Figure 11, an illustrative example displays the results for the 15 Hz sinusoid input signal, one of the ten measurements. The 15 Hz signal itself has no particular importance; the example just guides the reader through the method as the figure visualizes and explains what is meant under the specific metrics. Different subplots can be seen including raw time domain, amplitude spectrum, THD, SNR, SINAD, and SFDR for the prototype and Muse. On the other hand, Table 6 summarizes the mean and standard deviation (STD) values of the previously introduced metrics for all measurements.

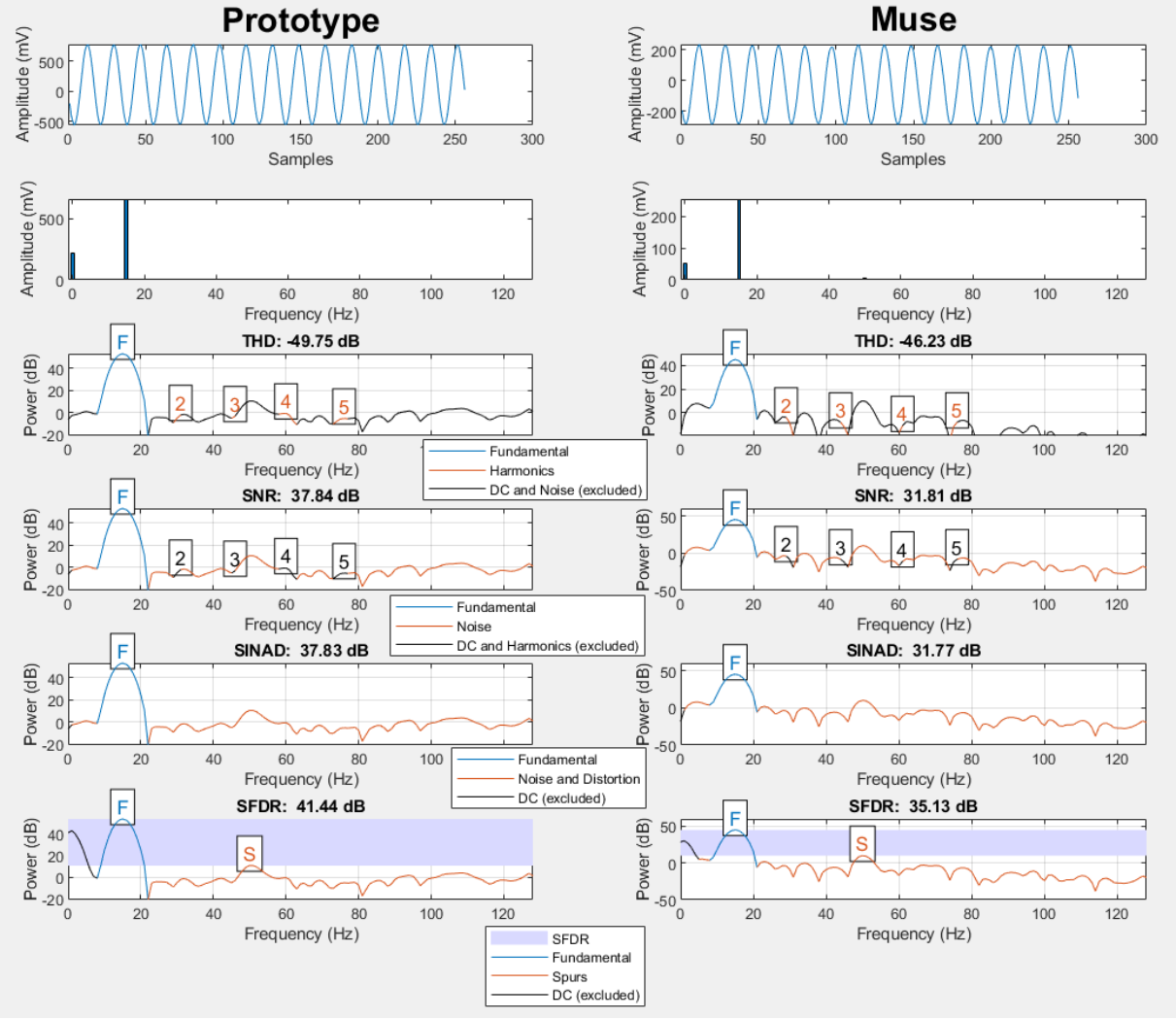

Figure 11 - Signal quality comparison of the devices for a 15 Hz sinusoid input signal. The left column belongs to the prototype, while the right belongs to Muse. The first row plots the raw time domain signal recorded for one second (256 samples at 256 Hz sampling frequency for both devices). The second row shows the amplitude spectra of the signals. The third row displays the Total Harmonic Distortion (THD), while the fourth shows the signals' Signal-to-Noise Ratio (SNR). The fifth row presents Signal-to-Noise and Distortion Ratio (SINAD), while the last row shows Spurious-free Dynamic Range (SFDR). The figure was created in MATLAB.

Table 6 - Summary of the signal quality metrics of the devices (mean and standard deviation)

Device	THD [dB]		SNR [dB]		SINAD [dB]		SFDR [dB]	
	Mean	*STD*	*Mean*	*STD*	*Mean*	*STD*	*Mean*	*STD*
Muse	-41.60	15.54	32.11	1.32	31.87	1.27	35.38	2.22
Prototype	-42.25	14.45	38.58	0.65	38.47	0.68	39.06	12.17

5.2 Physiological measurements

The purpose of the physiological measurements was to assess the effect of the artifacts on the EEG systems, particularly examining the mean changed power spectral density of specific brainwaves. There were four physiological measurements in total: breathing exercise, eye movement exercise, head movement exercise, and PASAT. The results were evaluated based on the grand mean of PSD values of theta, alpha, and beta bands. The mean PSD values were the inputs for the repeated measures ANOVA statistical analysis.

5.2.1 Breathing exercise

The Shapiro-Wilk test revealed that the averaged power spectral density values of the theta, alpha, and beta bands were normally distributed in the breathing exercise measurement. In the theta band, no significant main effect was observed when comparing the devices ($F_{(1,2)} = .412$, $p = .582$). However, a main effect of the breathing stimuli was observed, ($F_{(8,16)} = 2.864$, $p = .034$), indicating that the theta PSD was significantly altered by the controlled breathing pattern. No significant interaction effect was observed between the EEG devices and the breathing stimuli ($F_{(8,16)} = 1.446$, $p = .252$), revealing that EEG devices were comparable in detecting changes in PSD in the theta band.

In the alpha band, no significant main effect was observed when comparing the devices ($F_{(1,2)} = 4.625$, $p = .164$). No main effect of breathing cycles was observed ($F_{(8,16)} = 2.095$, $p = .099$), indicating that the alpha PSD is not significantly different across all breathing stimuli. No significant interaction effect was observed between the EEG devices and the breathing stimuli ($F_{(8,16)} = .221$, $p = .982$), revealing that EEG devices were comparable in detecting changes in PSD in the alpha frequency range. However, a pairwise comparison among the EEG devices revealed a significantly higher alpha PSD of the prototype compared to the Muse for 8 breathing cycles per minute ($F_{(1,2)} = 22.942$, $p = .042$) and 6 breathing cycles per minute ($F_{(1,2)} = 51.464$, $p = .019$).

In the beta band, no significant main effect was observed when comparing the devices ($F_{(1,2)} = 9.439$, $p = .092$); however, the sensitivity was approaching the significance level. The beta PSD values were not significantly affected by breathing stimuli ($F_{(8,16)} = .285$, $p = .961$). On the other hand, a significant interaction effect was observed between the EEG devices and the breathing stimuli ($F_{(8,16)} = 2.510$, $p = .056$)), revealing that EEG devices detected changes in PSD differently in the beta band. In more detail, a main effect of breathing stimuli was observed for the Muse ($F_{(1,2)} = 313.576$, $p = .040$). The mean PSD at various breathing rates for theta, alpha, and beta bands can be seen in Figure 12.

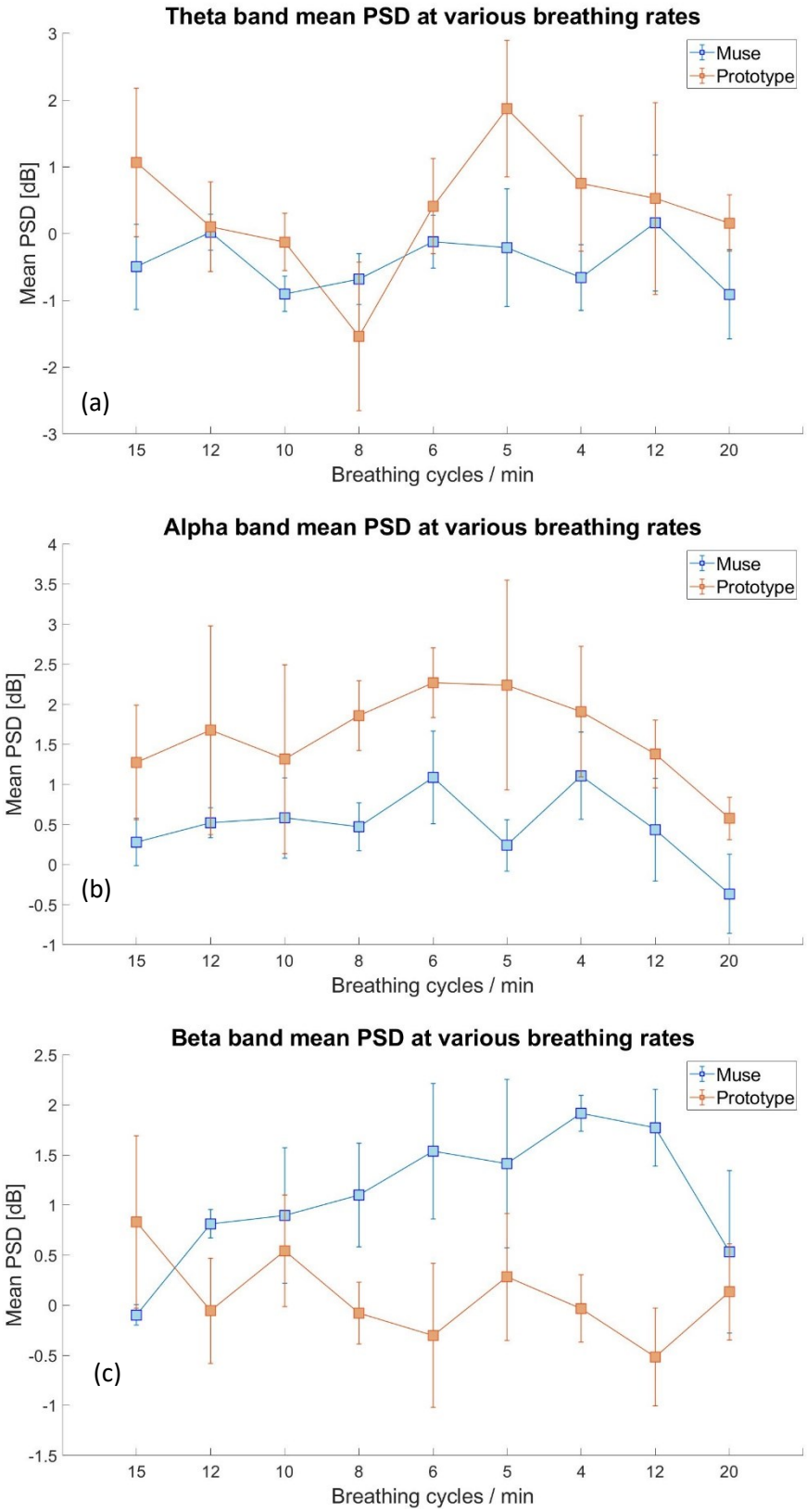

Figure 12 - Mean PSD at various breathing rates for theta (a), alpha (b), and beta (c) bands. The error bars represent standard errors. The sub-figures were taken from MATLAB.

5.2.2 Eye movement exercise

The Shapiro-Wilk test revealed that the averaged power spectral density values of the theta, alpha, and beta bands were normally distributed in the eye movement measurement. In the theta band, no significant main effect was observed when comparing the devices ($F_{(1,4)}$ = 3.409, p = .139). However, the theta PSD values were significantly altered by the eye movement stimuli ($F_{(2,8)}$ = 11.660, p = .004); therefore, theta could be a relevant indicator for eye movement artifacts. In more detail, a significantly increased theta PSD was observed in horizontal eye movement compared to circular (p = .005) and eye-closed (p = .06) conditions. A significant interaction effect was observed between the EEG devices and the eye movement stimuli ($F_{(2,8)}$ = 9.144, p = .009), revealing that EEG devices detected changes in PSD differently in the theta frequency range. In contrast, Muse had significantly lower theta PSD during horizontal eye movement than the prototype (p = .03).

In the alpha band, no significant main effect was observed when comparing the devices ($F_{(1,4)}$ = 4.355, p = .108). However, the alpha PSD values were significantly altered by eye movement stimuli $F_{(2,8)}$ = 12.443, p = .004); therefore, alpha could be a relevant indicator for the eye movement artifacts. A significant interaction effect was observed between the EEG devices and the eye movement stimuli ($F_{(2,8)}$ = 6.095, p = .025), revealing that EEG devices detected changes in PSD differently in the alpha band. In a more comprehensive comparison, the Muse had significantly lower alpha PSD during horizontal eye movement than the prototype (p = .024).

In the beta band, no significant main effect was observed when comparing the devices ($F_{(1,4)}$ = .027, p = .878). The beta PSD values were not significantly altered by eye movement stimuli ($F_{(2,8)}$ = 1.386, p = .304); therefore, beta could not be a relevant indicator for eye movement artifacts. No significant interaction effect was observed between the EEG devices and the eye movement stimuli ($F_{(2,8)}$ = 1.044, p = .395), revealing that EEG devices were comparable in detecting changes in PSD in the beta band. The mean PSD during various eye movement stimuli for theta, alpha, and beta bands can be seen in Figure 13.

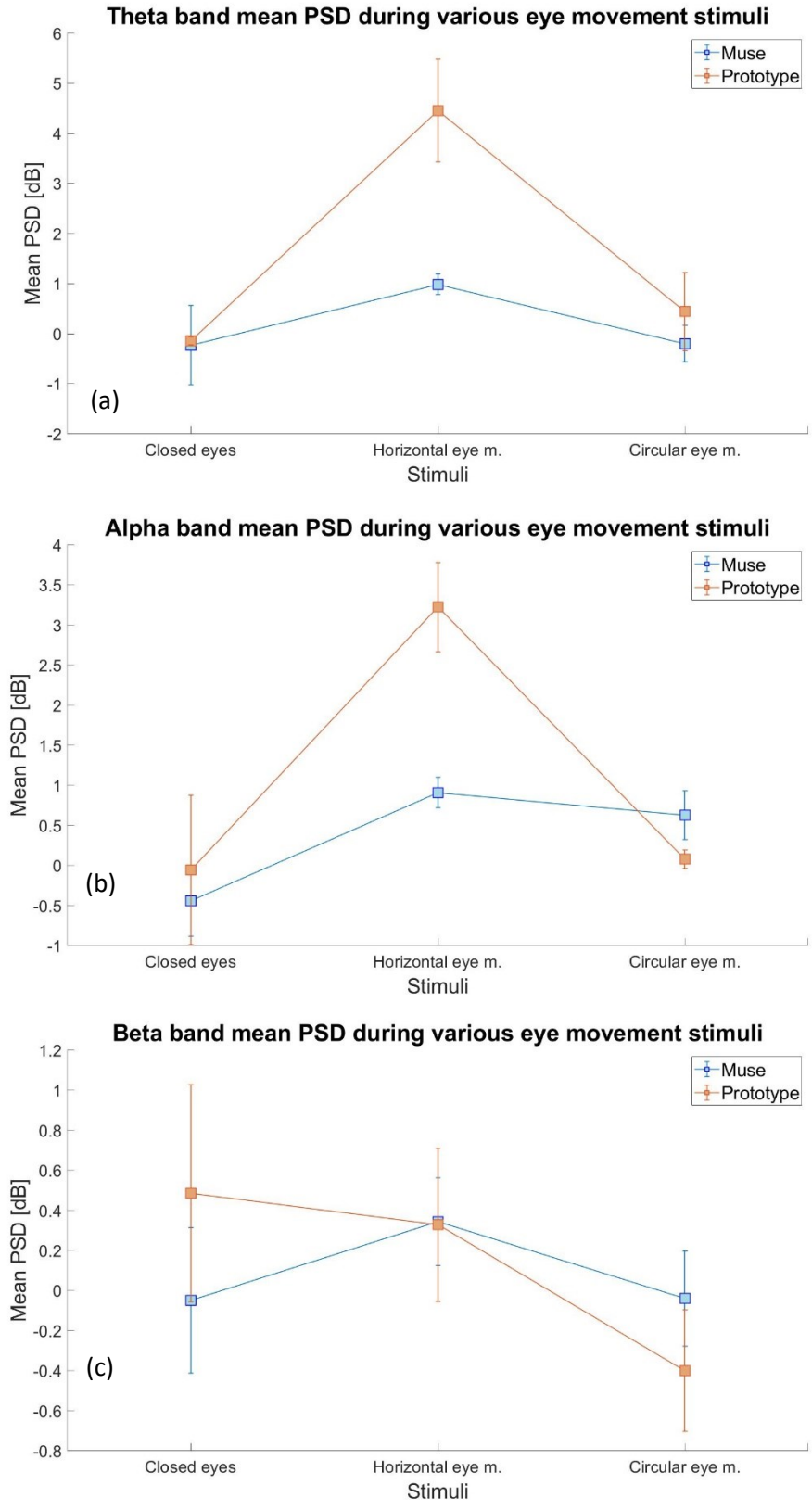

Figure 13 - Mean PSD during various eye movement stimuli for theta (a), alpha (b), and beta (c) bands. The error bars represent standard errors. The sub-figures were taken from MATLAB.

5.2.3 Head movement exercise

The Shapiro-Wilk test revealed that the averaged power spectral density values of the theta, alpha, and beta bands were normally distributed in the head movement measurement. In the theta band, no significant main effect was observed when comparing the devices ($F_{(1,2)} = .195$, $p = .702$). The theta PSD was not significantly altered by head movement stimuli ($F_{(2,4)} = 5.389$, $p = .079$); therefore, theta was not a relevant indicator for head movement artifacts. No significant interaction effect was observed between the EEG devices and the head movement stimuli ($F_{(2,4)} = .105$, $p = .902$), revealing that EEG devices were comparable in detecting changes in PSD in the theta band.

In the alpha band, no significant main effect was observed when comparing the devices ($F_{(1,2)} = 1.782$, $p = .314$). However, the alpha PSD was significantly altered by head movement stimuli ($F_{(2,4)} = 26.638$, $p = .005$); therefore, alpha could be a relevant indicator for head movement artifacts. No significant interaction effect was observed between the EEG devices and the head movement stimuli ($F_{(2,4)} = 1.223$, $p = .385$), revealing that EEG devices were comparable in detecting changes in PSD in the alpha frequency band.

In the beta band, no significant main effect was observed when comparing the devices ($F_{(1,2)} = .400$, $p = .592$). However, the beta PSD was significantly altered by head movement stimuli ($F_{(2,4)} = 22.113$, $p = .007$); therefore, beta could be a relevant indicator for head movement artifacts. Specifically, beta PSD was approaching a significantly lower intensity during roll compared to yaw ($p = 0.59$) and pitch ($p = .068$) head movements. No significant interaction effect was observed between the EEG devices and the head movement stimuli ($F_{(2,4)} = .086$, $p = .919$), revealing that EEG devices were comparable in detecting changes in PSD in the beta frequency band. The mean PSD during various head movement stimuli for theta, alpha, and beta bands can be seen in Figure 14.

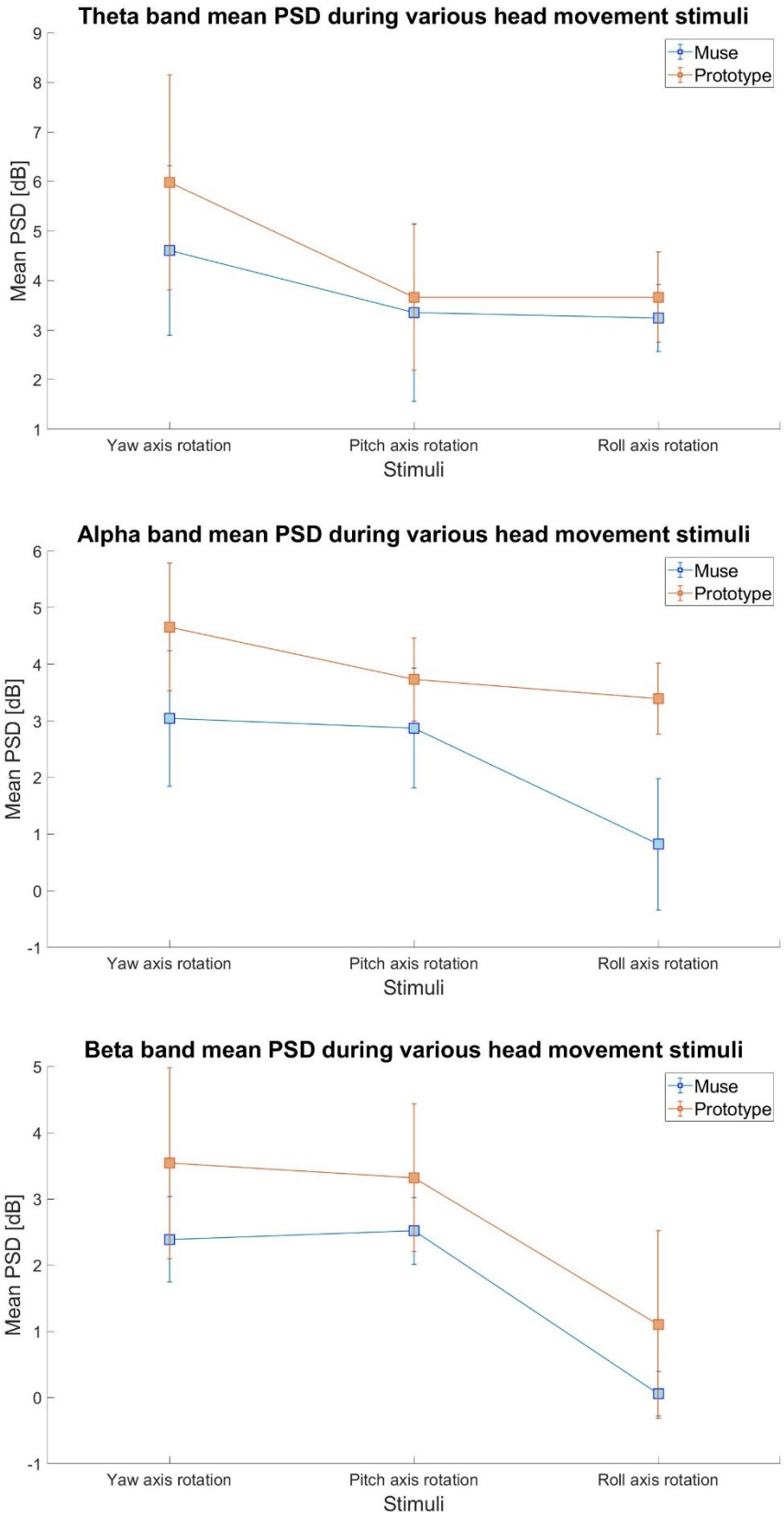

Figure 14 - Mean PSD during various head movement stimuli for theta (a), alpha (b), and beta (c) bands. The error bars represent standard errors. The sub-figures were taken from MATLAB.

5.2.4 Paced auditory serial addition test

The Shapiro-Wilk test revealed that the averaged power spectral density values of the theta, alpha, and beta bands were normally distributed in the PASAT measurement. However, the multivariate analysis of variance revealed that neither device was capable of detecting differences between the baseline and the PASAT, as neither main effect was significant in any frequency range: the theta band ($F_{(1,12)}$ = .010, p = .920), the alpha band ($F_{(1,12)}$ = .502, p = .492), and the beta band ($F_{(1,12)}$= .111, p = .744). The mean PSD difference between PASAT and baseline for theta, alpha, and beta bands can be seen in Figure 15.

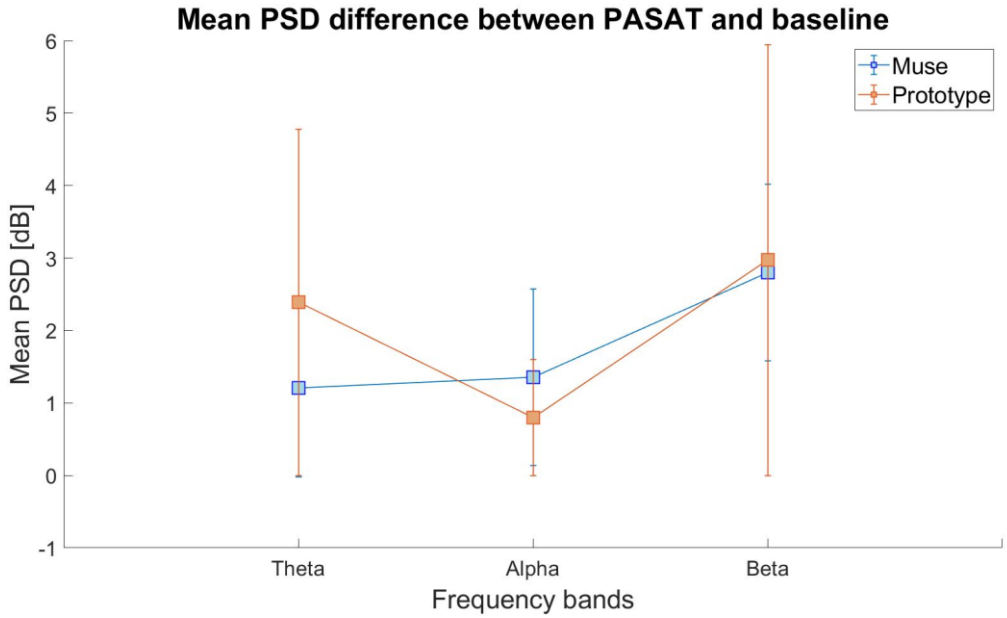

Figure 15 - Mean PSD difference between PASAT and baseline for theta, alpha, and beta bands. The error bars represent standard errors. The figure was taken from MATLAB.

Chapter 6

6 Discussion

The study aimed to validate the proposed prototype by comparing it against a commercial-grade EEG system, evaluate its suitability for neurofeedback, and explore design considerations for an affordable homecare BCI system. The comparison assessed the technical qualities of the devices while studying the sensitivity to fundamental brain activity and artifacts. Both devices were comparable in detecting changes brought on by the stimulations, there were some minor differences, however. The results served as a solid foundation for the discussion.

6.1 Technological considerations

When comparing the amplitude-frequency characteristics of the devices, it can be observed that Muse has a slightly downward-arched curve, and the most notable drops in amplitude are at both ends of the measured frequency range (at 3 and 60 Hz), where the amplitude drops up to 20% compared to the highest value. Meanwhile, the custom device has low-pass filter-like characteristics. In the lower frequency range, the amplitude is nearly constant, and it starts to drop around 20 Hz. The most notable drop in amplitude is less than 10% of the highest value located at 60 Hz. According to the datasheet of the instrumentation amplifier, the bandwidth (-3 dB) is 100 kHz at a given gain (10) [33]. Therefore, it is doubtful that this is the cause of the inclining; it probably originates from the artificial brain that added extra capacitive impedance to the system with the wet electrodes. One may suggest that the prototype's transfer characteristics are somewhat closer to the constant, distortionless transmission in the examined frequency range. However, only a narrow frequency band was examined (3-60 Hz) with limited frequency points.

As indicated by the results outlined above, Muse's average gain for ten samples was roughly 1000, while the prototype's mean gain was about 2900. The latter was around the geometric mean of the gain range since the prototype's gain is adjustable between 780 and 7800. Both devices' gain factors are deemed sufficient as the expected voltage range of neural oscillations is 10-100 µV [51]. The two devices' output is in the 0-5 V voltage range. Given that the input signals alternate, the highest amplitude without saturation can be a maximum of 2.5 V. However, the EEG Click's (the prototype's amplifier) virtual ground is set to be 2.048 V; therefore, the highest amplitude of the input can be roughly 2 V for the prototype when ignoring DC offsets for the sake of simplicity. The amplifier must be set carefully according to its output range and input range of the measurable signals because saturating the amplifier always yields information loss. During the physiological measurements, there were some cases when EEG Click's output was saturated for a few samples, in some extreme cases for a few seconds. In many cases, the affected epochs had to be rejected later because the useful signal could not be recovered. This issue could have been avoided by lowering the prototype's gain beforehand.

Besides the amplifier's gain factor, the ADC resolution plays a vital role in signal quality. In most cases, the operational amplifier SNR is usually much better than the analog-to-digital converter's SNR [52]. The microcontroller's ADC resolution is 10 bits; however, due to the most significant bit being the

sign bit, there are only 9 effective bits. Muse has 12 bits by default and 11 effective bits for similar considerations. According to the formula to calculate signal-to-noise ratio based on the number of ADC resolution bits [SNR (dB) = 6.02 x N + 1.76, where N denotes the number of bits], every new bit adds another 6 dB to the SNR [52]. Even if Muse's multi-channel advantage was not utilized to increase SNR, the signal quality properties of the two EEG devices were comparable, probably due to Muse's higher ADC resolution. Both devices' THD is slightly below -40 dB, roughly equivalent to 1% of harmonic distortion for the first five harmonics. Furthermore, the custom device is somewhat less sensitive to ambient noise, as the SNR and SINAD are 6 dB higher, while the SFDR is roughly 3 dB higher. The custom device performed just slightly better in the technical measurements regarding signal quality and amplitude-frequency characteristics. A possible takeaway for the prototype is to set a smaller gain for future measurements while increasing the overall SNR by selecting a microcontroller with a higher ADC resolution, for example, 12 or 14-bit.

Other differences in signal quality can originate from utilizing different types of electrodes. While Muse had dry electrodes, the prototype utilized wet electrodes. In contrast to dry electrodes, which are usually plain metal sheets, wet electrodes feature an electrolytic liquid, paste, or, most commonly, a gel between the skin and the metal electrode [53]. The usual assumption is that wet electrodes have higher SNR and less impedance, but some studies show that is only sometimes the case [54]. Dry electrodes are comparable in signal quality to wet electrodes. Wet electrodes' SNR tends to decrease as the gel dehydrates over time. The same study claims that dry electrodes are less affected by electromagnetic inference (EMI). The advantages of wet electrodes are that they typically offer more mechanical stability and flexibility with the electrode placement. Because of this, they are affected by motion artifacts less initially when the gel is fresh [54]. However, the artifact level increases as time passes, and the gel dehydrates. Besides, their drawbacks are that they are disposable and rather expensive: a bag of 10 electrode pads that were used cost €12. Since every measurement requires at least three new electrode pads, it is rather costly in the long haul, and their disposable nature also raises some sustainability and environmental questions. There is a third type of electrode called an insulating electrode. They are coupled capacitively to the body as opposed to the galvanic coupling of dry or wet electrodes, and this capacitive coupling is realized with dielectric film. These systems can acquire high-fidelity signals but require ultra-high input impedance amplifiers, biasing, guarding, and shielding techniques [53]. When using wet electrodes, the signal-to-noise ratio mainly depends on the electrode-skin interface. In contrast, in the case of the insulating electrodes, the SNR solely depends on the front-end circuit, where the noise of the amplifier is the critical factor. Utilizing insulating electrodes could increase the SNR; however, they would make the measurements even more complicated, inconvenient, and expensive. Therefore, they should not be used for homecare applications. On the other hand, switching from wet to dry electrodes could make the EEG headset more convenient, easier to set up, and cheaper. They are also more environmentally friendly than wet electrodes. Switching to dry electrodes is advised as it has more advantages than disadvantages for homecare applications.

As was stated before, the prototype has a single-channel EEG amplifier module. From a research perspective, obtaining better data goes beyond just higher signal quality, but also encompasses more complex data structures, such as recording from multiple electrode channels simultaneously. In general, larger electrode montages tend to yield better data as they have potentially more features. However, recent studies have highlighted the importance of considering the brain structure's uniqueness and diversity, as the subjects are the prominent source of variance [55]. Suggesting that smaller electrode montages with a larger pool of patients may lead to more valuable findings compared to larger montages with fewer patients in some cases. Therefore, even single-channel EEG systems can be relevant research tools for scientific studies. When considering treatment

purposes, the effectiveness of lower-density montages in EEG systems raises doubts. However, optimizing the lower number of electrodes can be still feasible for specific rehabilitation goals, while retaining the advantage of being more accessible to a wider population.

The sampling frequency of the prototype was chosen as 256 Hz, which was adequate for both long-term data acquisition and neurofeedback applications. Because of the Nyquist theorem, this sampling frequency allowed up to 128 Hz sample signals. Considering a 1-second time window, this yields a 1 Hz resolution. Since the study's upper frequency of interest was 60 Hz, even half of the sampling frequency would have been sufficient. Alternatively, half or a quarter of 1 sec would have been a sufficient time window for the FFT as the theta and alpha bands could be measured even with 4 Hz frequency resolution. Since the neurofeedback application was designed for a modern, multi-core PC (clock frequency around 3 Ghz) and the computational complexity of the FFT algorithm correlates to O (N log2(N), where N is the length of FFT input (in this case N is equal to 256), performing this computational task does not take much time and the application can be performed in real-time on the computer.

The prototype communicates through a USB cable, while the Muse transmits data through Bluetooth Classic. Wireless communication is arguably much more convenient and offers more flexibility, and most importantly directly promotes portability. On the other hand, this would also involve the integration of the battery into the prototype, and the new components would increase in size, weight, and cost. Nevertheless, the advantages still outweigh the disadvantages as adding the new components would improve comfort and user experience significantly. In the end, a wireless module, such as Bluetooth or Wi-Fi, and a battery pack should be added to the device, and a slightly bigger new headband should be designed for the prototype in this case. Although, the current-custom designed headband served its purpose. It is modular, can be assembled/disassembled for different configurations, and allows for adjustment of the position and height of the electrodes, offers considerable flexibility, while simultaneously holding the electrodes firmly. It is particularly designed to reduce the effect of movement-related artifacts and cable sway. The newer version of the headband should also possess these advantages.

6.2 Findings of the physiological assessment

Interpreting the results of the physiological measurements to draw clear conclusions can often be difficult in the field of EEG, as conclusions diverge in the specific literature in some cases [56]. This is primarily due to methodological choices but other factors such as qualities of the EEG system, number and placement of electrodes, mental state, brain structure, and other unique physiological differences of the test subjects can play a huge role in the outcome of the research [55]. In this study, simple commercial EEG systems were used with a limited number of electrodes and a small number of test subjects, in contrast to high-quality research studies with certified medical instruments and a larger number of participants. Nonetheless, some findings aligned with the widely accepted, mainstream literature.

In the breathing measurement, there were primarily similarities, with a few differences between the devices. Although the main effect for stimuli revealed that theta band was the only predictor of breathing artifacts, contrast results showed trends supporting the claim that alpha could also be a predictor. In the estimated marginal means figure (Figure 12), similar curves can be seen for the two devices. Both have downward arching curves indicating that as the breathing rate per minute

decreases, mean PSD in the alpha band increases and vice versa. The results align with the literature. According to most studies, a slower breathing rate correlates with increased alpha band power while decreased theta band power [56]. These brainwave changes are typically associated with increased relaxation and reduced alertness. Muse could distinguish between breathing rates in the beta band, while the prototype could not. Since the ground truth is not known, sensitivity in this band is not necessarily a good thing. Most likely, the difference is due to sampling error, as the power in the beta band should not increase based on the breathing rate theoretically. A possible takeaway can be the prototype is better suited to measure brain activity caused by the breathing exercise. In general, the measurement was according to the expectations.

The PASAT measurement did not yield any significant results. The aim of this measurement was to detect the altered brain activity induced by complex cognitive functions in the frontal lobe. Most likely, the method was not refined enough, the devices were not sensitive enough to detect meaningful differences in brain activity and the electrode placement was incorrect. This measurement needs to be thoroughly revised. Because of the quality of commercial devices, it was rather difficult to even distinguish fundamental brain activity from artifacts and noise. In the eye movement and head movement measurements, the assumption was that the detected changes in the power density spectra were due to artifacts and not because of altered brain activity. The available literature aims to prevent or remove artifacts rather than examine the changed spectrum.

The eye movement measurements revealed that theta and alpha bands were predictors of eye movement artifacts. Albeit the statistical analysis revealed the two devices behaved differently for the various stimuli as the interaction effects were significant in theta and alpha bands, conversely, the grand mean of the PSD values showed a similar "triangular, inverted V" pattern for both devices in these frequency ranges. In a manner, the two devices behaved similarly after all, but the extent of detecting the changes was statistically different. Nonetheless, the prototype detected lateral eye movement artifacts in the theta and alpha bands, while Muse did not. Lateral eye movement can distort the EEG recording, particularly affecting the outcome of neurofeedback to some degree [6]. This issue could be addressed by filtering out the ocular artifacts on the fly, for example with linear regression-based algorithms. The effect of blinking was not assessed during this study; however, it could be a possible future work. The subdivision of the frequency bands, especially the alpha band, would have been more conclusive. The findings were according to the expectations in general, which revealed that the prototype is more sensitive to eye movement artifacts. However, since no filtering mechanism was utilized, detecting eye movement artifacts were the expected and faithful result.

In the head movement measurements, an increased power could be observed throughout the whole spectrum for both devices due to the three head rotation stimuli. Only minor differences could be observed in the relative grand mean PSD of the devices, as the two devices behaved similarly in the three frequency bands for all stimuli. The results also revealed that alpha and beta bands were the predictors of head movement artifacts, while yaw and pitch axis rotation stimuli were the primary inducers of these artifacts. Artifacts caused by roll axis rotation were also present, but to a smaller extent, and the roll axis rotation was the least significant in the Beta band for both devices. Muse was somewhat less sensitive to the roll axis rotation. The measurements were according to the expectations as results showed both devices were affected by the head movements. The prototype was also expected to have slightly higher PSD due to the electrode cables, nevertheless, the headband remarkably held the cables firmly. A possible takeaway is that neither of the devices is good at detecting fundamental brain signals, particularly in the theta and alpha bands when head movements are present, e.g., during physical exercise. However, neurofeedback ideally requires a steady posture with little to no movement, sitting in front of the computer at home, where this is not an issue. Subtle

head and neck movement would affect the outcome of the neurofeedback to a minimal extent. To diminish the effect of these kinds of artifacts, gyroscope, and acceleration sensors could be utilized to assess the extent of the rotation, mark the temporal location of the artifacts in the recordings or disregard the affected brain activities. It is worth mentioning that Muse has both of the sensor types; however, it was not used during the measurement. This opens opportunities for further improvement in the methodology of the comparison and hardware of the prototype.

6.3 Impact of the study

The purpose of this project was to investigate how to develop a novel, custom, versatile, single-channel, portable EEG device from scratch for homecare neurofeedback. The EEG device was successfully realized and it could perform neurofeedback applications. The industrial impact of the project is laying down the foundation for the prototype, an MVP, which may become a product once. The custom device shows promise as an open-source EEG platform available for research purposes and may be implemented in future trials involving neurofeedback protocols. Nevertheless, the in-lab device needs a sizeable quality-of-life improvement beforehand, particularly to diminish the effects of artifacts.

The scientific interest of this project was investigating to design process, measuring the prototype's capabilities, and exploring its viability as an open-access research tool. The explorative study revealed that the in-lab device was comparable in technical properties to a commercial device, particularly in signal quality and robustness to artifacts. The study also investigated the relevant design considerations and usability requirements for a homecare neurofeedback BCI system. The project contributes to EEG research and development in the neurology and engineering fields. Therefore, the target audience of the study is electrical and medical engineers, EEG developers, technicians, neurology researchers, and clinicians. Besides that, anyone can benefit from reading the study who is interested in the development of a biomedical device prototype, commercial EEG device comparison, and validation, or neurofeedback.

The societal value of the project was that it supports the democratization of homecare by creating a device that enables the home treatment of motion sickness and visual vertigo. The demand for homecare is increasing, and this prototype may save time and energy for patients who require remote treatment. Therefore, energy saving is the primary impact regarded sustainability. Other aspects of sustainability to be evaluated can be the choice of materials for the EEG prototype. The device development was according to eco-consciousness and environmental awareness. The parts of the hardware components, such as integrated circuits and printed circuit boards, were chosen as most of them were made of Restriction of Hazardous Substances (RoHS) compliant materials. Besides, the headband was made of PLA, which is a biodegradable plastic material, created typically from fermented corn [57]. The least environmentally friendly and most questionable component of the EEG system was the disposable electrode pads, which were made of AgCl and unknown conductive and adhesive hydrogels [35]. Those electrode pads are expected to be replaced and thrown away after each EEG recording session. One should consider the energy consumption of the EEG system, although, it is negligible as it was designed for a few hours of training periods, and the estimated peak power consumption of the EEG system is less than 2 W. Regarding the price, the calculated current material cost of the prototype was around €85. Considering the aim for the democratization of homecare, a possible reasonable retail price for the future product should be no more than €170-200, ensuring a

maximum margin of 10-15%. This estimation takes into account expenses related to product development, labor, logistics, marketing, and other associated costs. Ideally, this consumer price would also include software packages, such as neurofeedback applications.

Ethical considerations involve the operation of the device, as the custom software handles personal data acquired from the brain waves during recording. If needed, the data can be stored locally without any kind of encryption. Personal data cannot be reached by unauthorized persons unless the patient is careless. Since EEG is a non-invasive method, theoretically, it would not harm the patient. In reality, however; there might be some leakage current during the operation of the EEG device which might be harmful. The effect and extent of this leakage current were not assessed during the project, as the amplifier was assumed to be compliant with the regulations. Finally, personal data was collected from 6 different subjects to perform the device comparisons during the project. The statistically processed data was published anonymously with the approval of the subjects, and the results cannot be traced back to individuals.

6.4 Limitations

The most significant limitation was the number of test subjects. As the sample size of the physiological measurements was small; it was difficult to draw clear conclusions. However, it was sufficient to create an explorative study. Due to some methodological considerations, only one of Muse's four active channels was recorded during the measurements. Ideally, all those channels should be recorded, and the relevant channels should be re-referenced, as this technique can significantly improve the SNR. Another possible limitation was not choosing the best reference point for the electrodes. For simplicity reasons, the custom device had the reference electrode at a similar position as the Muse. An alternative choice for the prototype's reference would have been either the mastoid or the earlobe, but further research is recommended to investigate this. Lastly, measurements were affected by EMI, and this should have been avoided by having higher fidelity results. Because of the quality and grade of the devices, the ground truth of the fundamental brain could have not been determined properly which questions the validity of the results. Besides, the examination of the artifacts has been beed defined too vaguely, and improperly. The amplitude–frequency characteristics were more precisely frequency-limited, real value transfer characteristics. During the study, only a narrow frequency band was examined (3-60 Hz) with limited frequency points, and only amplitude information was preserved; therefore, the phase information of the complex transfer characteristic was excluded from the comparison.

Chapter 7

7 Conclusion

The low-cost, portable, single-channel, custom EEG system was successfully designed, developed, and realized. Supporting software for a computer, including an EEG data recorder and a neurofeedback demo application, was implemented. Primary objective I. of the thesis completed. The prototype was compared to Muse, a commercial-grade meditative EEG system validated for scientific research beforehand. Addressing the research aim, the two devices were comparable in technical properties, particularly in signal quality and robustness to artifacts. The prototype had a slightly higher, roughly 6 dB higher signal-to-noise ratio in a general sense, and had a more flat amplitude-frequency characteristic. The study remains inconclusive as to what extent the devices were affected by artifacts because the sample size was too small and there was no ground truth for measuring the artifacts. However, the conclusion can be that it is worth investigating this matter further and conducting more refined and complex measurements in the future. The prototype seemed more affected by eye movement artifacts as meaningful changes could be seen in its spectrum by horizontal eye movement stimuli, which could distort the fundamental signal. On the other hand, both devices were affected by head movement artifacts, but this is probably not an issue from the aspect of the target application, neurofeedback. The usability requirements have been identified for the NFB BCI system, and some possible improvements were suggested for design considerations. A possible takeaway is that prototype is suitable for neurofeedback in the theta band now, and after some ocular artifact filtering is implemented, the prototype will be primed for neurofeedback in the alpha band as well. Another suggestion is converting the communication wireless, to make the BCI fully portable and improve convenience during homecare use. Primary objective II. of the thesis is considered to be achieved. Lastly, the neurofeedback application could replay a POV roller coaster video at a varying frame rate, whose feedback value was based on the theta band's mean PSD. As was stated earlier, the neurofeedback ran on the prototype successfully. The secondary objective of the thesis was achieved, therefore, all three objectives of the thesis have been accomplished.

To summarize, the prototype meets the technical requirements, is comparable to Muse in its qualities, has the expected behavior about physiological changes, and is capable of performing neurofeedback, yet the material cost is roughly one-third of Muse's consumer price. Therefore, the in-lab device is deemed to be validated and the minimal viable product is considered to be achieved. The final verdict is that the custom device shows promise as an open-source EEG platform, and there is a good possibility that the prototype's successor can become a homecare product one day as the foundation of the device has been laid down successfully. However, beforehand, the in-lab device needs some improvements to diminish the effects of artifacts, increase the resolution of the analog-to-digital converter, transform the communication into wireless, and replace the wet electrodes with dry ones. So whether the prototype becomes a product or not is a matter of resources from now.

7.1 Future work

A portion of the future work should address the limitations and mistakes mentioned in the previous section, which essentially means improving the method. The first step can be extending the explorative study to draw more definite and accurate conclusions. As was stated earlier, the most significant issue with the measurement was the too-small sample size. For future work, conducting a more diverse physiological measurement with more human subjects, such as 30-50 people, with a broader set of stimuli and more refined methods, is suggested. The latter involves that the investigated brainwaves can be subdivided into smaller frequency ranges, such as alpha (8-12 Hz) subdivided into alpha1 (8-10 Hz), alpha2 (10-12 Hz), and alpha3 (12-13 Hz). The measurements should also be conducted under a more controlled environment, especially to reduce electromagnetic inference. Use of EMC shielded isolation chamber or room is advised. The prototype could be compared against a certificated medical device to determine ground truth and draw more accurate conclusions. Furthermore, different functionalities of the device should be assessed, for example, to determine whether it is capable of ERP-related research. In addition, more thorough technical measurements could be conducted to measure the internal noise of the amplifier which can also be a relevant metric for determining signal quality. Finally, the effects of other artifacts not discussed in this project, such as electrocardiography (ECG), pulse, or tremor artifacts, should be investigated in future work [6].

Besides the method, the prototype itself could be improved in many ways, mostly hardware-wise, such as replacing the current analog-to-digital converter with a higher resolution one, converting the communication wireless, and replacing wet electrodes with dry electrodes. The amplifier was sufficient in terms of signal quality; however, it could be replaced with a multi-channel amplifier. This would enhance the capabilities of the devices as well as increase signal quality. Furthermore, because of the multi-channel extension, the number and position of the electrodes should be revised. The headband could be redesigned to match the new electrode number or improve general comfort. Finally, the prototype could be equipped with gyroscope and accelerometer sensors which could help to filter out movement-based artifacts.

The neurofeedback application could also be enhanced significantly. Based on the rollercoaster POV video, a procedurally generated neurofeedback „videogame” could be developed. The graphical elements, such as textures and 2D or even 3D models, would be generated based on patterns of brainwaves. The transformed feedback would rely on the PSD values of more refined frequency ranges, such as theta 1, theta 2, alpha 1, alpha 2, and alpha 3. This multivariate input would offer custom-tailored, unique solutions for each subject instead of a flat, unchanging video. Alternatively, the application could also include an audio signal besides visual feedback to extend the affected senses. Finally, the neurofeedback application should be validated at some point, by performing weeks-long training sessions on several test subjects.

8 References

[1] M. Kiss, *Demographic Outlook for the European Union 2020*, no. March. 2020. Accessed: Mar. 03, 2023. [Online]. Available: https://epthinktank.eu/2022/06/03/demographic-outlook-for-the-european-union-2022/

[2] R. Tarricone and A. D. Tsourus, *Home care in Europe. The solid facts*. 2008.

[3] N. Genet *et al.*, "Home care in Europe: A systematic literature review," *BMC Health Serv. Res.*, vol. 11, 2011, doi: 10.1186/1472-6963-11-207.

[4] H. Peng, B. Hu, Y. Qi, Q. Zhao, and M. Ratcliffe, "An improved EEG de-noising approach in electroencephalogram (EEG) for home care," *2011 5th Int. Conf. Pervasive Comput. Technol. Healthc. Work. PervasiveHealth 2011*, pp. 469–474, 2011, doi: 10.4108/icst.pervasivehealth.2011.246021.

[5] J. Haueisen, P. Fiedler, A. Bernhardt, R. Gonçalves, and C. Fonseca, "Novel dry electrode EEG headbands for home use: Comparing performance and comfort," *Curr. Dir. Biomed. Eng.*, vol. 6, no. 3, pp. 0–3, 2020, doi: 10.1515/cdbme-2020-3036.

[6] M. OSTOW, *Clinical electroencephalography*, vol. 9, no. 11–12. 2009. doi: 10.1212/wnl.23.7.782.

[7] P. Sawangjai, S. Hompoonsup, P. Leelaarporn, S. Kongwudhikunakorn, and T. Wilaiprasitporn, "Consumer Grade EEG Measuring Sensors as Research Tools: A Review," *IEEE Sens. J.*, vol. 20, no. 8, pp. 3996–4024, 2020, doi: 10.1109/JSEN.2019.2962874.

[8] Mayo Clinic, "EEG (electroencephalogram) - Mayo Clinic," *EEG - Tests and procedures*, 2020. https://www.mayoclinic.org/tests-procedures/eeg/about/pac-20393875 (accessed Sep. 02, 2022).

[9] S. Gill and O. Sumant, "2019 ELECTROENCEPHALOGRAPHY (EEG) EQUIPMENT MARKET," no. December, pp. 1–72, 2019.

[10] Polaris Market Research, "Electroencephalography Devices Market," 2022.

[11] G. Sintotskiy and H. Hinrichs, "In-ear-EEG–a portable platform for home monitoring," *J. Med. Eng. Technol.*, vol. 44, no. 1, pp. 26–37, Jan. 2020, doi: 10.1080/03091902.2020.1713238.

[12] A. Martín-Araguz, C. Bustamante-Martínez, M. T. Emam-Mansour, and J. M. Moreno-Martínez, "Neuroscience in ancient Egypt and in the school of Alexandria," *Revista de Neurologia*, vol. 34, no. 12. pp. 1183–1194, 2002. doi: 10.33588/rn.3412.2001461.

[13] M. N. Hart, "The Origins of Neuroscience. A History of Explorations into Brain Function," *J. Neuropathol. Exp. Neurol.*, vol. 53, no. 5, pp. 545.2-545, 1994, doi: 10.1097/00005072-199409000-00015.

[14] T. Mahfoud, S. McLean, and N. S. Rose, "Vital models : the making and use of models in the brain sciences," vol. 233, no. 17, p. 226, 2016.

[15] I. B. Levitan and L. K. Kaczmarek, *The Neuron*. Oxford University Press, 2015. doi: 10.1093/med/9780199773893.001.0001.

[16] S. Stern, A. Rotem, Y. Burnishev, E. Weinreb, and E. Moses, "External excitation of neurons

using electric and magnetic fields in one- and two-dimensional cultures," *J. Vis. Exp.*, vol. 2017, no. 123, May 2017, doi: 10.3791/54357.

[17] L. Vasung *et al.*, "Exploring early human brain development with structural and physiological neuroimaging," *Neuroimage*, vol. 187, pp. 226–254, Feb. 2019, doi: 10.1016/j.neuroimage.2018.07.041.

[18] G. Thierry, "Neurophysiological examination methods: Electrophysiology and neuroimaging," in *Cognitive Neurology: A Clinical Textbook*, Oxford University Press, 2012. doi: 10.1093/acprof:oso/9780198569275.003.0003.

[19] M. Carter and J. Shieh, *Guide to Research Techniques in Neuroscience, Second Edition*. Elsevier, 2015. doi: 10.1016/C2013-0-06868-5.

[20] Queensland University, "How to measure brain activity in people - Queensland Brain Institute - University of Queensland," *https://qbi.uq.edu.au/*. https://qbi.uq.edu.au/brain/brain-functions/how-measure-brain-activity-people (accessed Sep. 16, 2022).

[21] T. C. Ferree, M. T. Clay, and D. M. Tucker, "The spatial resolution of scalp EEG," *Neurocomputing*, vol. 38–40, pp. 1209–1216, Jun. 2001, doi: 10.1016/S0925-2312(01)00568-9.

[22] G. H. Glover, "Overview of functional magnetic resonance imaging," *Neurosurgery Clinics of North America*, vol. 22, no. 2. NIH Public Access, pp. 133–139, Apr. 2011. doi: 10.1016/j.nec.2010.11.001.

[23] P. A. Abhang, B. W. Gawali, and S. C. Mehrotra, *Technological Basics of EEG Recording and Operation of Apparatus*. 2016. doi: 10.1016/b978-0-12-804490-2.00002-6.

[24] A. D. Legatt, "Evoked Potentials," in *Encyclopedia of the Neurological Sciences*, Elsevier Inc., 2014, pp. 228–231. doi: 10.1016/B978-0-12-385157-4.00529-7.

[25] *Encyclopedia of Clinical Neuropsychology*. Springer New York, 2011. doi: 10.1007/978-0-387-79948-3.

[26] S. Michelmann *et al.*, "Data-driven re-referencing of intracranial EEG based on independent component analysis (ICA)," *J. Neurosci. Methods*, vol. 307, pp. 125–137, Sep. 2018, doi: 10.1016/j.jneumeth.2018.06.021.

[27] J. J. Shih, D. J. Krusienski, and J. R. Wolpaw, "Brain-computer interfaces in medicine," *Mayo Clinic Proceedings*, vol. 87, no. 3. Mayo Foundation, pp. 268–279, 2012. doi: 10.1016/j.mayocp.2011.12.008.

[28] D. C. Hammond, "What is neurofeedback?," *Journal of Neurotherapy*, vol. 10, no. 4. pp. 25–36, 2006. doi: 10.1300/J184v10n04_04.

[29] O. M. Giggins, U. M. C. Persson, and B. Caulfield, "Biofeedback in rehabilitation," *Journal of NeuroEngineering and Rehabilitation*, vol. 10, no. 1. BioMed Central, pp. 1–11, Jun. 18, 2013. doi: 10.1186/1743-0003-10-60.

[30] H. Marzbani, H. R. Marateb, and M. Mansourian, "Methodological note: Neurofeedback: A comprehensive review on system design, methodology and clinical applications," *Basic Clin. Neurosci.*, vol. 7, no. 2, pp. 143–158, Mar. 2016, doi: 10.15412/j.bcn.03070208.

[31] AVR Studio®, "ATmega328P 8-bit AVR Microcontroller with 32K Bytes In-System Programmable Flash DATASHEET," *ATmega328P [DATASHEET]*, pp. 6–288, 2016, [Online]. Available: https://ww1.microchip.com/downloads/en/DeviceDoc/Atmel-7810-Automotive-Microcontrollers-ATmega328P_Datasheet.pdf

[32] MikroElektronika, “EEG Click | Mikroe,” 2022. https://www.mikroe.com/eeg-click (accessed Jan. 17, 2023).

[33] Burr Brown, “INA114 Data Sheet,” 1998, [Online]. Available: http://pdf1.alldatasheet.com/datasheet-pdf/view/56674/BURR-BROWN/INA114.html

[34] M. Guermandi, E. F. Scarselli, and R. Guerrieri, “A Driving Right Leg Circuit (DgRL) for Improved Common Mode Rejection in Bio-Potential Acquisition Systems,” *IEEE Trans. Biomed. Circuits Syst.*, vol. 10, no. 2, pp. 507–517, Apr. 2016, doi: 10.1109/TBCAS.2015.2446753.

[35] Covidien, “Kendall ™ ECG Electrodes Product Data Sheet,” vol. 44, no. 0, p. 1, 2008.

[36] J. Kowaleski, “BlueMuse: Windows 10 app to stream data from Muse EEG headsets via LSL (Lab Streaming Layer).” https://github.com/kowalej/BlueMuse (accessed Apr. 16, 2023).

[37] Theme Park Review [YouTube], “Steel Dragon 2000 Roller Coaster POV Awesome 4K Ultra HD Resolution Nagashima Spaland Japan.” 2015. Accessed: Apr. 16, 2023. [Online]. Available: https://www.youtube.com/watch?v=5WrRDN6gGvM

[38] “MBC - Marianne Bernadotte Centrum | Karolinska Institutet.” https://ki.se/cns/mbc-marianne-bernadotte-centrum (accessed Aug. 22, 2022).

[39] R. Rahma and J. Nurhadi, “Measurement of Concentration Duration on Reading Activity: EEG Analysis with OpenBCI Ganglion Board,” *SSRN Electron. J.*, 2017, doi: 10.2139/ssrn.3174465.

[40] K. Permana, S. K. Wijaya, and P. Prajitno, “Controlled wheelchair based on brain computer interface using Neurosky Mindwave Mobile 2,” in *AIP Conference Proceedings*, Nov. 2019, vol. 2168, no. 1, p. 020022. doi: 10.1063/1.5132449.

[41] O. E. Krigolson, C. C. Williams, A. Norton, C. D. Hassall, and F. L. Colino, “Choosing MUSE: Validation of a low-cost, portable EEG system for ERP research,” *Front. Neurosci.*, vol. 11, no. MAR, p. 109, Mar. 2017, doi: 10.3389/fnins.2017.00109.

[42] “OpenBCI | Home.” https://openbci.com/about (accessed Mar. 20, 2023).

[43] “Ganglion Board (4-channels) – OpenBCI Online Store.” https://shop.openbci.com/products/ganglion-board (accessed Mar. 20, 2023).

[44] InteraXon, “Muse 2: Brain Sensing Headband - Technology Enhanced Meditation,” 2020. https://choosemuse.com/muse-2/ (accessed Mar. 20, 2023).

[45] “MindWave.” https://store.neurosky.com/pages/mindwave (accessed Mar. 21, 2023).

[46] Ó. K. RÚNARSSON, “Using EEG in neurofeedback training to decrease visual motion sensitivity and motion-sickness,” KTH Royal Institute of Technology, 2021.

[47] C. Cannard, H. Wahbeh, and A. Delorme, “Validating the wearable MUSE headset for EEG spectral analysis and Frontal Alpha Asymmetry,” in *Proceedings - 2021 IEEE International Conference on Bioinformatics and Biomedicine, BIBM 2021*, 2021, pp. 3603–3610. doi: 10.1109/BIBM52615.2021.9669778.

[48] C. Simar, M. Petieau, A. Cebolla, A. Leroy, G. Bontempi, and G. Cheron, “EEG-based brain-computer interface for alpha speed control of a small robot using the MUSE headband,” Jul. 2020. doi: 10.1109/IJCNN48605.2020.9207486.

[49] W. Kester, “Understand SINAD, ENOB, SNR, THD, THD+ N, and SFDR so You Don’t Get Lost in the Noise Floor,” *Analog Devices Tutorial, MT-003, Rev. A*, pp. 2–9, 2009, [Online]. Available: http://instrumentation.analog.com/static/imported-files/tutorials/MT-003.pdf

[50] T. N. Tombaugh, “A comprehensive review of the Paced Auditory Serial Addition Test (PASAT),” *Arch. Clin. Neuropsychol.*, vol. 21, no. 1, pp. 53–76, 2006, doi: 10.1016/j.acn.2005.07.006.

[51] C. Fu, S. Lin, and N. Sada, “Portable EEG Device to Assist with Sleep Disorders”.

[52] B. Carter, P. Rowland, J. Karki, and P. Miller, “Amplifier and Bits: An Introduction to Selecting Amplifiers for Data Converters,” *Texas Instruments Appl. Report, …*, no. December, pp. 1–27, 2001, [Online]. Available: http://scholar.google.com/scholar?hl=en&btnG=Search&q=intitle:Amplifiers+and+Bits+:+An+Introduction+to+Selecting+Amplifiers+for+Data+Converters#7

[53] E. Spinelli and M. Haberman, “Insulating electrodes: A review on biopotential front ends for dielectric skin-electrode interfaces,” *Physiol. Meas.*, vol. 31, no. 10, 2010, doi: 10.1088/0967-3334/31/10/S03.

[54] A. Searle and L. Kirkup, “A direct comparison of wet, dry and insulating bioelectric recording electrodes,” *Physiol. Meas.*, vol. 21, no. 2, pp. 271–283, 2000, doi: 10.1088/0967-3334/21/2/307.

[55] A. Melnik *et al.*, “Systems, subjects, sessions: To what extent do these factors influence EEG data?,” *Front. Hum. Neurosci.*, vol. 11, p. 150, Mar. 2017, doi: 10.3389/fnhum.2017.00150.

[56] A. Zaccaro *et al.*, “How Breath-Control Can Change Your Life: A Systematic Review on Psycho-Physiological Correlates of Slow Breathing,” *Frontiers in Human Neuroscience*, vol. 12. 2018. doi: 10.3389/fnhum.2018.00353.

[57] B. Bax and J. Müssig, “Impact and tensile properties of PLA/Cordenka and PLA/flax composites,” *Composites Science and Technology*, vol. 68, no. 7–8. Elsevier, pp. 1601–1607, Jun. 01, 2008. doi: 10.1016/j.compscitech.2008.01.004.